$Ru(CO)_4(PMe_2Ph)$ Catalyzed Carbonylation of $Ru(CH_3)I(CO)_2$(iPr-DAB) and $Ru(CH_3)I(CO)_2$(iPr-Pyca) Complexes. X-ray Structure of [$Ru(CH_3)(CO)_2$[(2-methoxyethyl)Pyca]][OTf]

Barbara de Klerk-Engels, Johannes H. Groen, Marco J. A. Kraakman, Jan Meine Ernsting, and Kees Vrieze*

Anorganisch Chemisch Laboratorium, Universiteit van Amsterdam, Nieuwe Achtergracht 166, 1018 WV Amsterdam, The Netherlands

Kees Goubitz and Jan Fraanje

Laboratorium voor Kristallografie, Universiteit van Amsterdam, Nieuwe Achtergracht 166, 1018 WV Amsterdam, The Netherlands

Received January 28, 1994®

The synthesis and characterization of complexes $Ru(R)X(CO)_2(R'$-Pyca) (R = CH_3 and X = I (**2**); R = $C(O)CH_3$ and X = I (**3**); R = CH_3 and X = OTf = SO_3CF_3 (**4**); R = $C(O)CH_3$ and X = OTf (**5**); R^1-Pyca = 2-R^1-pyridinecarbaldimine; and R′ = isopropyl (**b**), methoxyethyl (**c**), or isopropoxypropyl (**d**)), respectively, will be presented. The X-ray structure determination of the yellow crystals of [$Ru(CH_3)(CO)_2(CH_3OCH_2CH_2$-Pyca)][OTf] (**4c**) has been carried out. Crystal data for **4c**: monoclinic, space group $P2_1/c$ with a = 8.5008(4) Å, b = 12.3281(8) Å, c = 18.412(1) Å, β = 101.118(6)°, V = 1893.4(2) Å^3, Z = 4. The $Ru(CO)_4(PMe_2Ph)$ (**13**) catalyzed CO insertion in the methyl–ruthenium bond of $Ru(CH_3)X(CO)_2$(iPr-DAB) (X = I (**2a**); X = OTf (**4a**); X = Cl (**6a**); DAB = 1,4-diaza-1,3-butadiene) and $Ru(CH_3)X(CO)_2$(iPr-Pyca) (X = I (**2b**); X = OTf (**4b**)) has been studied by use of labeled $Ru(^{13}CO)_4(PMe_2Ph)$ (**13**) and by reaction in the absence or presence of additional ligand PPh_3 and CO. For the neutral complexes **2a**, **6a**, and **2b** the key intermediate for the CO insertion catalyzed by **13** is most probably of the type [$Ru(CH_3)X(CO)$(α-diimine)$Ru(CO)_3(PMe_2Ph)(\mu$-$CO)_2$] (**X1**), which is, however, not observed during the reaction. By ^{13}CO labeling experiments it has clearly been demonstrated that binuclear species are involved in this reaction. Complex $Ru(CO)_4$-(PMe_2Ph) (**13**) decomposes in $CDCl_3$ at 45 °C under N_2 and under a CO atmosphere (1 and 8 atm) within 3 h to form $Ru_2(CO)_4(PMe_2Ph)_2(\mu$-$Cl)_2$ (**15**), which can further react with PPh_3 to $Ru_2(CO)_4(PMe_2Ph)_2(PPh_3)_2(\mu$-$Cl)_2$ (**16**). Suprisingly, **13** is stable under high CO pressure in the presence of **2a**, **6a**, and **2b** in $CDCl_3$ at 45 °C for several hours, most probably as a result of a faster reaction of $Ru(CO)_4(PMe_2Ph)$ (**13**) or most likely [$Ru(CO)_3(PMe_2Ph)$] with **2a**, **6a**, or **2b** than with $CDCl_3$, which prohibits decomposition.

Introduction

The migratory insertion of carbon monoxide in metal–carbon bonds has been extensively studied in the last decades since it is an essential feature of many important industrial processes.[1-4] Most of the systems studied up till now involve a metal carbonyl species with an alkyl group which reacts with free CO.[3,4] Reactions in which another metal complex is the carbonyl source or even catalyzes the carbonylation are much less common.[5]

Recently, Kraakman et al. published the acylation reaction of $Ru(CH_3)I(CO)_2$(iPr-DAB) (**2a**) to form $Ru(C(O)CH_3)I(CO)_2$(iPr-DAB) (**3a**) at 45 °C, which was catalyzed by $Ru(CO)_4(PR_3)$.[6] A very interesting feature is that the acylation is very much enhanced by increasing donor capacities of PR_3 and does not correlate with its cone angle. In this study we restrict ourselves to the use of $Ru(CO)_4(PMe_2Ph)$ (**13**), since **13** was proven to be the most efficient catalyst.[6]

It was proposed that complexes **2a** and **13** are in equilibrium with a binuclear species **X1** (step i in Scheme 1).[6] The exact structure of the intermediate **X1** is not known, but the fact that CO scrambling between **2a** and **13** takes place suggested a structure with

* To whom correspondence should be addressed.

® Abstract published in *Advance ACS Abstracts,* July 1, 1994.

(1) Falbe, J., Ed. *New Syntheses with Carbon Monoxide*; Springer-Verlag: Berlin, 1980.

(2) See for example: (a) Parshall, G. W. *Homogeneous Catalysis: The Applications and Chemistry of Catalysis by Soluble Transition Metal Complexes*; Wiley-Interscience: New York, 1980 (see also references cited therein). (b) Happel, J.; Umemura, S.; Sakakibara, Y.; Blanck, H.; Kunichika, S. *Ind. Eng. Chem. Proc. Des. Dev.* **1975**, *14*, 44.

(3) See refs 1 and 2. (a) Paulik, F. E. *Catal. Rev.* **1972**, *6*, 49. (b) Kuntz, E. G.; *CHEMTECH.* **1987**, Sept, 570. (c) Drent, E. Eur. Pat. Appl. 271144, 1988. (d) Drent, E.; Budzelaar, P. H. M.; Jager, W. W.; Stapersma, J. Eur. Pat. Appl. 441447, 1991. (e) Drent, E.; van Broekhoven, J. A. M.; Doyle, M. J. *J. Mol. Catal.* **1991**, *417*, 235. (f) Slaugh, L. H.; Mullinaux, R. D. U.S. Pat. 3,239,569, 1966. (g) Slaugh, L. H.; Mullinaux, R. D. U.S. Pat. 3,239,570, 1966.

(4) Calderazzo, F. *Angew. Chem.* **1977**, *89*, 305.

(5) (a) Rosen, R. P.; Hoke, J. B.; Whittle, R. R.; Geoffroy, G. L.; Hutchinson, J. P.; Zubieta, J. A. *Organometallics* **1984**, *3*, 846. (b) LaCroce, S. J.; Cutler, A. R. *J. Am. Chem. Soc.* **1982**, *104*, 2312.

(6) Kraakman, M. J. A.; de Klerk-Engels, B.; de Lange, P. P. M.; Vrieze, K.; Smeets, W. J. J.; Spek, A. L. *Organometallics* **1992**, *11*, 3774.

0276-7333/94/2313-3279$04.50/0

Scheme 1. Proposed Mechanism for the $Ru(CO)_4(PMe_2Ph)$ (13) Assisted CO Insertion in $Ru(CH_3)I(CO)_2$(iPr-DAB) (2a) in the Presence of L and C–H Activation in the Absence of L[6]

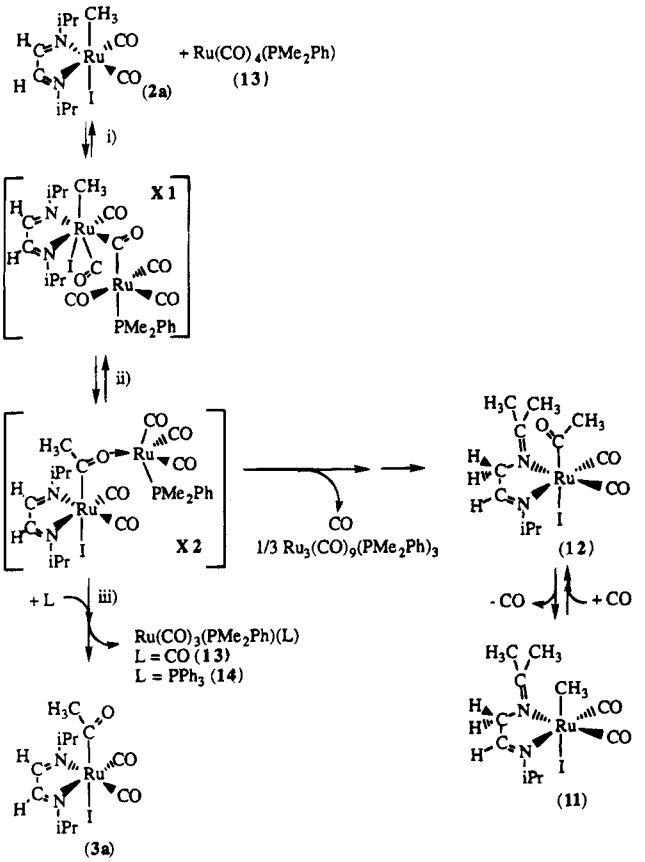

bridging CO ligands. In the second step (ii) nucleophilic attack of the methyl group on one of the carbonyl groups takes place, forming **X2**. In analogy to recent reported bimetallic compounds stabilized by bridging acyl groups the unsaturated $Ru(CO)_3(PMe_2Ph)$ fragment in **X2** is stabilized by the acyl function.[7] Subsequent addition of L (step iii) yields $Ru(C(O)CH_3)I(CO)_2$(iPr-DAB) (**3a**) and $Ru(CO)_3(PMe_2Ph)(L)$ (L = CO (**13**), PPh_3 (**14**)). Under a CO atmosphere the reaction is catalytic, because complex **13** is formed again after carbonylation by addition of CO (Scheme 1).[6] If neither CO nor PPh_3 was added to **2a** and **13**, a mixture of complexes $Ru(CH_3)I(CO)_2(iPrN{=}C(H)CH_2N{=}C(CH_3)_2)$ (**11**) and $Ru(C(O)CH_3)I(CO)_2(iPrN{=}C(H){-}CH_2N{=}C(CH_3)_2)$ (**12**) was formed, as a result of C–H activation.[6,8]

Since the $Ru(CO)_4(PMe_2Ph)$ (**13**) assisted acylation reaction of **2a** is one of the few examples of acylation catalyzed via bimetallic intermediates, we decided to direct our attention to the further elucidation of the mechanism of this reaction. To this end, we replaced the symmetric iPr-DAB ligand by the asymmetric R′-Pyca (Pyca = pyridinecarbaldimine) ligand. As it is known that subtle changes of the R group of α-diimine ligands can have a large influence on the stability of the metal complex and its reactivity, we varied the R′ group in R′-Pyca.[9] In Figure 1 the ligands iPr-DAB (**a**) and R′-Pyca with R′ = iPr (**b**), $CH_3OCH_2CH_2$ (**c**), and $iPrOCH_2CH_2CH_2$ (**d**) are depicted.

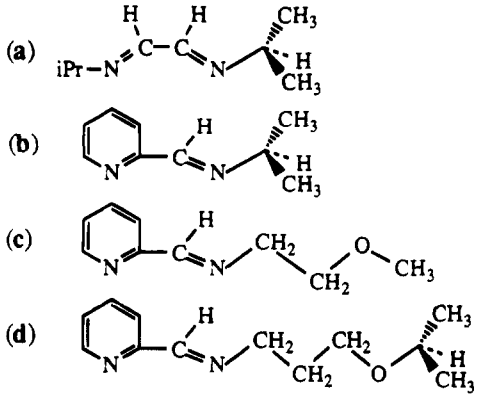

Figure 1. Ligands iPr-DAB (**a**), iPr-Pyca (**b**), $CH_3OCH_2CH_2$-Pyca (**c**), and $CH(CH_3)_2OCH_2CH_2CH_2$-Pyca (**d**).

Experimental Section

$RuCl_3{\cdot}3H_2O$ was obtained as a loan from Johnson Matthey, Inc. Complexes $RuI_2(CO)_2$(iPr-DAB) (**1a**),[10] $Ru(CH_3)I(CO)_2$(iPr-DAB) (**2a**),[10] [$Ru(CH_3)(CO)_2$(iPr-DAB)][OTf] (**4a**),[6] $RuI_2(CO)_2$(iPr-Pyca) (**1b**),[10] $Ru(CH_3)I(CO)_2$(iPr-Pyca) (**2b**),[10] and $Ru(CO)_4(PMe_2Ph)$ (**13**)[6,11] were prepared as described before. Ligands $CH_3OCH_2CH_2$-Pyca (**c**) and $iPrOCH_2CH_2CH_2$-Pyca (**d**) were prepared according to ref 12. Unless stated otherwise, all syntheses were carried out under an atmosphere of dry nitrogen, using standard Schlenk techniques. Solvents were dried by refluxing over sodium or calcium carbonate. Column chromatography was performed using dried and activated silica gel (Kieselgel 60, E. Merck, 70–238 mesh) as the stationary phase. ^1H, ^{13}C, and ^{31}P NMR measurements were carried out on a Bruker AMX 300 spectrometer (300.13, 75.46, and 121.51 MHz, respectively) at 293 K unless stated otherwise. Chemical shifts (δ, ppm) are given relative to $SiMe_4$. IR spectra were recorded on a Perkin-Elmer 283 spectrometer. Field desorption (FD) mass spectra were obtained with a Varian MAT711 double focusing mass spectrometer with a combined EI/FI/FD source, fitted with a 10-μm tungsten wire FD-emitter containing carbon microneedles with an average length of 30 μm, using emitter currents of 0–15 mA. Elemental analyses were carried out by Dornis und Kolbe, Mikroanalytisches Laboratorium, Mülheim a.d. Ruhr, Germany. The products were identified by elemental analysis, ^1H, ^{13}C, and ^{31}P NMR, and IR spectroscopy.

Synthesis of $Ru(CH_3)I(CO)_2$(R′-Pyca) (2) and $Ru(C(O)CH_3)I(CO)_2$(R′-Pyca) (3). Complexes **2** and **3** for iPr-DAB (**a**) were prepared by the method reported by Kraakman et al.[6]

(7) (a) Carmona, E.; Munoz, M. A.; Rogers, R. D. *Inorg. Chem.* **1988**, *27*, 1598. (b) Sünkel, K.; Nagel, U.; Beck, W. *J. Organomet. Chem.* **1983**, *251*, 227. (c) See ref 5.

(8) Mul, W. P.; Elsevier, C. J.; Vrieze, K.; Smeets, W. J. J.; Spek, A. L. *Organometallics* **1992**, *11*, 1891.

(9) (a) van Koten, G.; Vrieze, K. In *Advances in Organometallic Chemistry*; Stone, F. G. A., West, R. Eds.; Academic Press: New York, 1982; Vol. 21, p 151. (b) Vrieze, K. *J. Organomet. Chem.* **1986**, *300*, 307. (c) Muller, F.; van Koten, G.; Vrieze, K.; Heijdenrijk, D.; *Organometallics* **1989**, *8*, 33. (c) Muller, F.; van Koten, G.; Polm, L. H.; Vrieze, K.; Zoutberg, M. C.; Heijdenrijk, D.; Kragten, E.; Stam, C. H. *Organometallics* **1989**, *8*, 1340.

(10) (a) Kraakman, M. J. A.; Vrieze, K.; Kooijman, H.; Spek, A. L. *Organometallics* **1992**, *11*, 3760. (b) The acyl complex $Ru(C(O)CH_3)I(CO)_2$(iPr-DAB) (**3a**) is only formed when the solution is refluxed in heptane instead of hexane. However, complex $Ru(C(O)CH_3)I(CO)_2$(iPr-Pyca) (**3b**) is formed in 10–15% yield in hexane, but this compound was not isolated by Kraakman using this synthesis because column chromatography was stopped too early (elution with CH_2Cl_2).

(11) (a) Johnson, B. F. G.; Lewis, J.; Twigg, M. V. *J. Chem. Soc., Dalton Trans.* **1975**, 1876. (b) L'Eplattenier, F.; Calderazzo, F. *Inorg. Chem.* **1968**, *7*, 1290.

(12) de Klerk-Engels, B.; Frühauf, H.-W.; Vrieze, K.; Kooijman, H.; Spek, A. L. *Inorg. Chem.* **1993**, *32*, 5528.

1b/2b/3b. **1b** and **2b** were obtained as described.[6] Ru(C(O)CH$_3$)I(CO)$_2$(iPr-Pyca) (**3b**) was obtained in the third fraction (elution CH_2Cl_2/Et_2O = 1/1) in 10% yield. Data for **3b**: IR (CH_2Cl_2) ν(CO) 2041 (s), 1980 (s), cm^{-1}; ^{1}H NMR ($CDCl_3$) δ 1.43, 1.54 (d, J = 6.6 Hz, 6H, CH(C*H*$_3$)$_2$), 2.51 (s, 3H, Ru—C(O)C*H*$_3$), 4.24 (sept, J = 6.6 Hz, 2H, C*H*(CH$_3$)$_2$), 7.44 (m, 1H, py H5), 7.95 (m, 1H, py H3), 8.02 (m, 1H, py H4), 8.48 (s, 1H, N=C(*H*)), 8.81 (d, 5.1 Hz, 1H, py H6); ^{13}C NMR ($CDCl_3$) δ 23.8, 23.9 (CH(*C*H$_3$)$_2$), 49.5 (Ru—C(O)*C*H$_3$), 65.8 (*C*H(CH$_3$)$_2$), 127.2 (py C5), 128.8 (py C4), 149.2 (py C3), 152.7 (py C6), 155.0 (py C2), 162.7 (N=CH), 200.0, 200.6 (CO's), 242.4 (Ru—*C*(O)CH$_3$).

1c/2c/3c. Using the same procedure starting with $Ru_3(CO)_{12}$ (345 mg, 0.54 mmol), $CH_3OCH_2CH_2$-Pyca (**c**) (394 mg, 2.40 mmol), and MeI (excess) **1c**, **2c**, and **3c** were obtained in 10, 80, and 10% yields, respectively. Data for $RuI_2(CO)_2(CH_3OCH_2CH_2$-Pyca) (**1c**) are as reported.[12] Data for Ru(CH$_3$)I(CO)$_2$(CH$_3$OCH$_2$CH$_2$-Pyca) (**2c**): IR (CH_2Cl_2) ν(CO) 2029 (s), 1965 (s) cm^{-1}; ^{1}H NMR ($CDCl_3$) δ 0.04 (s, 3H, Ru—CH$_3$), 3.37 (s, 3H, OC*H*$_3$), 3.79–3.88 and 3.92–3.99 (m, 2H, NCH$_2$C*H*$_2$O), 4.14–4.23 and 4.31–4.4 (m, 2H, NC*H*$_2$CH$_2$O), 7.53 (m, 1H, py H5), 7.89 (d, J = 7.5 Hz, 1H, py H3), 7.99 (m, 1H, py H4), 8.34 (s, 1H, N=C(*H*)), 8.97 (d, J = 4.5 Hz, 1H, py H6); ^{13}C NMR ($CDCl_3$) δ −5.4 (Ru—CH$_3$), 59.2 (O*C*H$_3$), 64.6 and 69.8 (N*C*H$_2$CH$_2$O and NCH$_2$*C*H$_2$O), 128.0 (py C5), 128.8 (py C4), 149.0 (py C3), 153.1 (py C6), 153.6 (py C2), 164.8 (N=CH), 202.4, 202.7 (CO's). Data for Ru(C(O)CH$_3$)I(CO)$_2$(CH$_3$OCH$_2$CH$_2$-Pyca) (**3c**): IR (CH_2Cl_2) ν(CO) 2042 (s), 1980 (s) cm^{-1}; ^{1}H NMR ($CDCl_3$) δ 2.43 (s, 3H, Ru—C(O)CH$_3$), 3.32 (s, 3H, OC*H*$_3$), 3.64–3.72 and 3.85–3.94 (m, 2H, NCH$_2$C*H*$_2$O), 4.11–4.20 (m, 2H, NC*H*$_2$CH$_2$O), 7.45 (m, 1H, py H5), 7.94 (d, J = 7.5 Hz, 1H, py H3), 7.99 (m, 1H, py H4), 8.43 (s, 1H, N=C(*H*)), 8.80 (d, J = 5.4 Hz, 1H, py H6); ^{13}C NMR ($CDCl_3$) δ 48.2 (C(O)*C*H$_3$), 58.5 (O*C*H$_3$), 63.5 and 69.5 (N*C*H$_2$CH$_2$O and NCH$_2$*C*H$_2$O), 126.9 (py C5), 128.4 (py C4), 138.7 (py C3), 152.2 (py C6), 154.0 (py C2), 166.2 (N=CH), 199.2, 199.3 (CO's), 240.95 (Ru—*C*(O)CH$_3$). Anal. Calcd for $C_{12}H_{15}N_2O_3RuI$: C, 31.11; H, 3.26; N, 6.04%. Found: C, 31.19; H, 3.31; N, 5.96.

1d/2d/3d. The same procedure starting with $Ru_3(CO)_{12}$ (99 mg, 0.15 mmol), $CH(CH_3)_2OCH_2CH_2CH_2$-Pyca (**d**) (150 mg, 0.73 mmol), and MeI (excess), produced **1d**, **2d**, and **3d** in 10, 75, and 15% yields, respectively.

Data for $RuI_2(CO)_2(CH(CH_3)_2OCH_2CH_2$-Pyca) (**1d**) are as reported.[12] Data for Ru(CH$_3$)I(CO)$_2$(CH(CH$_3$)$_2$-OCH$_2$CH$_2$CH$_2$-Pyca) (**2d**): IR (CH_2Cl_2) ν(CO) 2030 (s), 1963 (s) cm^{-1}; ^{1}H NMR ($CDCl_3$) δ 0.04 (s, 3H, Ru—CH$_3$), 1.13 and 1.17 (d, J = 6.6 Hz, 6H, CH(C*H*$_3$)$_2$), 2.13–2.41 (m, 2H, CH$_2$C*H*$_2$CH$_2$), 3.43–3.62 (m, 3H, NCH$_2$CH$_2$C*H*$_2$O and C*H*(CH$_3$)$_2$), 2.13–2.41 (m, 2H, CH$_2$C*H*$_2$CH$_2$), 3.43–3.62 (m, 3H, NCH$_2$CH$_2$C*H*$_2$O and C*H*(CH$_3$)$_2$), 4.13–4.40 (m, 2H, NC*H*$_2$CH$_2$CH$_2$O), 7.52 (dd, J = 7.5 and 5.4 Hz, 1H, py H5), 7.85 (d, J = 7.5 Hz, 1H, py H3), 7.99 (dd, J = 7.5 and 7.5 Hz, 1H, py H4), 8.36 (s, 1H, N=C(*H*)), 8.99 (d, J = 5.4 Hz, 1H, py H6); ^{13}C NMR ($CDCl_3$) δ −5.2 (Ru—CH$_3$), 22.7 and 22.8 (CH(*C*H$_3$)$_2$), 30.5 (CH$_2$*C*H$_2$CH$_2$), 62.5 (NCH$_2$), 64.5 (OCH$_2$), 72.1 (*C*H(CH$_3$)$_2$), 127.9 (py C5), 128.4 (py C4), 138.9 (py C3), 153.1 (py C6), 153.6 (py C2), 164.6 (N=CH), 202.3, 202.5 (CO's). Anal. Calcd for $C_{15}H_{21}N_2O_3RuI$: C, 35.65; H, 4.19; N, 5.54. Found: C, 35.74; H, 4.13, N, 5.46. Data for Ru(C(O)-CH$_3$)I(CO)$_2$(CH(CH$_3$)$_2$OCH$_2$CH$_2$CH$_2$-Pyca) (**3d**): IR (CH_2Cl_2): ν(CO) 2040 (s), 1980 (s) cm^{-1}; ^{1}H NMR ($CDCl_3$) δ 1.15 and 1.16 (d, J = 6.6 Hz, 6H, CH(C*H*$_3$)$_2$), 1.94–2.26 (m, 2H, CH$_2$C*H*$_2$CH$_2$), 2.48 (s, 3H, Ru—C(O)C*H*$_3$), 3.39–3.62 (m, 3H, NCH$_2$CH$_2$C*H*$_2$O and C*H*(CH$_3$)$_2$), 4.03–4.30 (m, 2H, NC*H*$_2$CH$_2$CH$_2$O), 7.47 (dd, J = 7.8 and 5.1 Hz, 1H, py H5), 7.92 (d, J = 7.8 Hz, 1H, py H3), 8.03 (dd, J = 7.8 and 7.8 Hz, 1H, py H4), 8.39 (s, 1H, N=C(*H*)), 8.83 (d, J = 5.1 Hz, 1H, py H6); ^{13}C NMR ($CDCl_3$) δ 22.9 (CH(*C*H$_3$)$_2$), 30.7 (CH$_2$*C*H$_2$CH$_2$), 49.6 (Ru—C(O)*C*H$_3$), 62.5 (NCH$_2$), 64.6 (OCH$_2$), 72.3 (*C*H(CH$_3$)$_2$), 127.3 (py C5), 128.7 (py C4), 139.4 (py C3), 153.2 (py C6), 155.1 (py C2), 165.8 (N=CH), 200.2, 200.3 (CO's). Anal. Calcd for $C_{16}H_{21}N_2O_4RuI$: C, 36.03; H, 3.97; N, 5.25. Found: C, 35.48; H, 4.24; N, 5.55.

Conversion of Ru(C(O)CH$_3$)I(CO)$_2$(iPr-Pyca) (3b) to Ru(CH$_3$)I(CO)$_2$(iPr-Pyca) (2b). A solution of Ru(C(O)CH$_3$)I(CO)$_2$(iPr-Pyca) (**3b**) (110 mg, 0.23 mmol) in 50 mL of heptane was refluxed for 18 h. After evaporation of the solvent Ru(CH$_3$)I(CO)$_2$(iPr-Pyca) (**2b**) resulted in quantitative yield, as revealed by ^{1}H and ^{31}P NMR.

Reaction of Ru(CH$_3$)I(CO)$_2$(iPr-Pyca) (2b) with PPh$_3$. A solution of Ru(CH$_3$)I(CO)$_2$(iPr-Pyca) (**2b**) (10 mg, 0.02 mmol) and PPh_3 (excess) in 0.5 mL of $CDCl_3$ was stirred for 1 h at 20 °C. No reaction occurred, as revealed by ^{1}H and ^{31}P NMR. At 45 °C circa 10% of **2b** had converted to [Ru(CH$_3$)(CO)$_2$(iPr-Pyca)(PPh$_3$)][I] (**8b**) after 4 h, as revealed by ^{1}H and ^{31}P NMR.

Synthesis of [Ru(CH$_3$)(CO)$_2$(R′-Pyca)][OTf] (4). 4b. To a yellow solution of Ru(CH$_3$)I(CO)$_2$(iPr-Pyca) (**2b**) (1–6 mg, 0.24 mmol) in 25 mL of THF was added AgOTf (66 mg, 0.26 mmol). After stirring for 15 min at 20 °C the light yellow solution was filtered. Evaporation of the solvent yielded **4b** in quantitative yield. IR (CH_2Cl_2): ν(CO) 2044 (s), 1975 (s) cm^{-1}. ^{1}H NMR ($CDCl_3$): δ 0.07 (s, 3H, Ru—CH$_3$), 1.50, 1.52 (d, J = 6.5 Hz, 6H, CH(C*H*$_3$)$_2$), 4.26 (sept, J = 6.5 Hz, 2H, C*H*(CH$_3$)$_2$), 7.66 (m, 1H, py H5), 7.94 (d, J = 7.5 Hz, 1H, py H3), 8.10 (m, 1H, py H4), 8.60 (s, 1H, N=C(*H*)), 8.95 (d, J = 4.5 Hz, 1H, py H6). ^{13}C NMR ($CDCl_3$): δ −15.2 (Ru—CH$_3$), 23.1, 23.4 (CH(*C*H$_3$)$_2$), 65.8 (*C*H(CH$_3$)$_2$), 129.1 (py C5), 129.4 (py C4), 140.5 (py C3), 153.4 (py C6), 154.4 (py C2), 166.3 (N=CH), 199.1, 199.8 (CO's).

4c. The same procedure described as above, starting with **2c** (145 mg, 0.29 mmol) and AgOTf (76 mg, 0.30 mmol), resulted in formation of **4c** in quantitative yield. Crystals of **4c** were obtained from a concentrated CH_2Cl_2/hexane mixture (10/1) at −20 °C. Data for [Ru(CH$_3$)(CO)$_2$(CH$_3$OCH$_2$CH$_2$-Pyca)][OTf] (**4c**): IR (CH_2Cl_2) ν(CO) 2042 (s), 1964 (s) cm^{-1}; ^{1}H NMR ($CDCl_3$) δ 0.006 (s, 3H, Ru—C*H*$_3$), 3.38 (s, 3H, OC*H*$_3$), 3.74–3.90 (m, 2H, NCH$_2$C*H*$_2$O), 4.10–4.35 (m, 2H, NC*H*$_2$CH$_2$O), 7.68 (m, 1H, py H5), 7.92 (d, J = 9.0 Hz, 1H, py H3), 7.11 (m, 1H, py H4), 8.48 (s, 1H, N=C(*H*)), 8.93 (d, J = 4.5 Hz, 1H, py H6); ^{13}C NMR ($CDCl_3$) δ −15.2 (Ru—CH$_3$), 59.2 (O*C*H$_3$), 64.0 and 69.1 (N*C*H$_2$CH$_2$O and NCH$_2$*C*H$_2$O), 128.6 (py C5), 129.3 (py C4), 140.6 (py C3), 153.5 (py C6), 154.1 (py C2), 168.5 (N=CH), 199.1, 199.4 (CO's).

4d. The same procedure starting with **2d** resulted in decomposition of the product.

Synthesis of [Ru(C(O)CH$_3$)(CO)$_2$(R′-Pyca)][OTf] (5). 5b. A yellow solution of [Ru(CH$_3$)(CO)$_2$(iPr-Pyca)][OTf] (**4b**) (62 mg, 0.09 mmol) was placed under a CO atmosphere. After stirring for 15 min at 20 °C and evaporation of the solvent, **5b** resulted in quantitative yield. IR (CH_2Cl_2): ν(CO) 2055 (s), 1992 (s) cm^{-1}. ^{1}H

NMR ($CDCl_3$): δ 1.40, 1.42 (d, J = 6.1 Hz, 6H, CH(CH_3)$_2$), 2.42 (s, 3H, Ru—acyl), 4.19 (sept, J = 6.1 Hz, 2H, C*H*(CH_3)$_2$), 7.61 (m, 1H, py H5), 7.98 (d, J = 5.2 Hz, 1H, py H3), 8.11 (m, 1H, py H4), 8.62 (s, 1H, N=C(*H*)), 8.82 (d, J = 4.48 Hz, 1H, py H6). ^{13}C NMR ($CDCl_3$): δ 22.5, 26 (CH(CH_3)$_2$), 48.3 (Ru—C(O)CH_3), 64.9 (*C*H(CH_3)$_2$), 128.1 (py C5), 128.5 (py C4), 140.4 (py C3), 152.6 (py C6), 154.7 (py C2), 165.7 (N=CH), 196.5, 197.2 (CO's), 235.1 (Ru—*C*(O)CH_3).

5c. The same procedure for [Ru(CH_3)(CO)$_2$($CH_3OCH_2CH_2$-Pyca)][OTf] (**4c**) (50 mg, 0.07 mmol) yielded **5c** in quantitative yield. Data for [Ru(C(O)CH_3)(CO)$_2$($CH_3OCH_2CH_2$-Pyca)][OTf] (**5c**): IR (CH_2Cl_2) ν(CO) 2059 (s), 1993 (s) cm^{-1}; ^1H NMR ($CDCl_3$) δ 2.43 (s, 3H, Ru—C(O)C*H*$_3$), 3.32 (s, 3H, OC*H*$_3$), 3.64—3.72 and 3.85—3.94 (m, 2H, NCH_2CH_2O), 4.11—4.20 (m, 2H, NCH_2CH_2O), 7.45 (m, 1H, py H5), 7.94 (d, J = 7.5 Hz, 1H, py H3), 7.99 (m, 1H, py H4), 8.43 (s, 1H, N=C(*H*)), 8.80 (d, J = 5.4 Hz, 1H, py H6); ^{13}C NMR ($CDCl_3$) δ 48.2 (C(O)*C*H$_3$), 58.5 (O*C*H$_3$), 63.5 and 69.5 (NCH_2CH_2O and NCH_2CH_2O), 126.9 (py C5), 128.4 (py C4), 138.7 (py C3), 152.2 (py C6), 154.0 (py C2), 166.2 (N=CH), 199.2, 199.3 (CO's), 240.95 (Ru—*C*(O)CH_3).

Synthesis of [Ru(CH_3)(CO)$_2$(PPh_3)(iPr-Pyca)][OTf] (9b). To a solution of [Ru(CH_3)(CO)$_2$(iPr-Pyca)][OTf] (**4b**) (15 mg, 0.03 mmol) in 25 mL of dichloromethane was added PPh_3 (9 mg, 0.04 mmol). After stirring for 10 min at 20 °C, the solvent was evaporated and the residue washed with hexane (10 mL). The residue yielded **9b** in quantitative yield. IR (CH_2Cl_2): ν(CO) 2042 (s), 1984 (s) cm^{-1}. ^1H NMR ($CDCl_3$): δ 0.19 (d, J(P—H) = 3.9 Hz, 3H, Ru—C*H*$_3$), 0.99, 1.30 (d, J = 6.3 Hz, 6H, CH(C*H*$_3$)$_2$), 3.96 (sept, J = 6.3 Hz, 2H, C*H*(CH_3)$_2$), 7.1—7.6 (m, 16H, P*Ph* and py H5), 8.00 (m, 2H, py H3 and py H4), 8.85 (d, J = 7.8 Hz, 1H, py H6), 9.05 (d, J(P—H) = 2.7 Hz, 1H, N=C(*H*)). ^{31}P NMR ($CDCl_3$): δ 21.9.

Synthesis of [Ru(C(O)CH_3)(CO)$_2$(PPh_3)(iPr-Pyca)][OTf]. To a solution of [Ru(C(O)CH_3)(CO)$_2$(iPr-Pyca)][OTf] (**5b**) (40 mg, 0.08 mmol) in 25 mL of dichloromethane was added PPh_3 (18 mg, 0.08 mmol). After stirring for 10 min at 20 °C, the solvent was evaporated and the residue washed with hexane (10 mL). The residue yielded [Ru(C(O)CH_3)(CO)$_2$(PPh_3)(iPr-Pyca)][OTf] in quantitative yield. ^1H NMR ($CDCl_3$): δ 0.97, 1.07 (d, J = 6.6 Hz, 6H, CH(C*H*$_3$)$_2$), 2.62 (s, Ru—C(O)C*H*$_3$), 3.76 (sept, J = 6.6 Hz, 2H, C*H*(CH_3)$_2$), 7.0—7.4 (m, 16H, P*Ph* and py H5), 7.90 (d, J = 5.4 Hz, 1H, py H3 or py H4), 8.00 (t, J = 6.0 Hz, 1H, py H3 or py H4), 8.87 (d, J = 7.8 Hz, 1H, py H6), 9.06 (d, J(P—H) = 2.7 Hz, 1H, N=C(*H*)). ^{31}P NMR ($CDCl_3$): δ 18.2.

Reaction of $RuI_2(CO)_2$(iPr-DAB) (1a) with Ru(^{13}CO)$_4$(PMe_2Ph) (13). (i) A solution of **1a** (5 mg, 0.01 mmol) and Ru(^{13}CO)$_4$(PMe_2Ph) (**13**) (5 mg, 0.014 mmol) in 0.5 mL of $CDCl_3$ was placed in an NMR tube. The reaction was monitored with ^1H, ^{13}C, and ^{31}P NMR: after 8 h at 20 °C 50% of Ru(^{13}CO)$_4$(PMe_2Ph) (**13**) was converted to **15**. No ^{13}CO enrichment of **1a** had taken place.

(ii) A solution of **1a** (12 mg, 0.02 mmol) and Ru(^{13}CO)$_4$(PMe_2Ph) (**13**) (6 mg, 0.02 mmol) in 50 mL of CH_2Cl_2 was refluxed for 3 h. After evaporation of the solvent ^{13}C NMR showed that **1a** was enriched with ^{13}CO.

Reactions of Ru(CH_3)I(CO)$_2$(iPr-DAB) (2a). (i) With Ru(CO)$_4$(PMe_2Ph) and PPh_3. (ia) A solution of Ru(CH_3)I(CO)$_2$(iPr-DAB) (**2a**) (6 mg, 0.02 mmol), Ru(CO)$_4$(PMe_2Ph) (**13**) (6 mg, 0.02 mmol), and PPh_3 (4 mg, 0.015 mmol) in 0.5 mL of $CDCl_3$ was placed in an NMR tube. The reaction was monitored with ^1H and ^{31}P NMR: after 20 h at 20 °C no reaction had taken place; at 45 °C 71% of **2a** was converted to Ru(C(O)CH_3)I(CO)$_2$(iPr-DAB) (**3a**) and 2% of **13** was converted to [Ru(CO)$_2$(PMe_2Ph)Cl]$_2$ (**15**) after 17 h.

(ib) In THF at 45 °C (**2a** 9 mg, 0.02 mmol; **13** 9 mg, 0.03 mmol; PPh_3 8 mg, 0.03 mmol) complex **13** was totally converted to Ru(CO)$_3$(PMe_2Ph)(PPh_3) (**14**) after 2 h, with only 5% conversion of **2a** to **3a**.

(ii) With PPh_3. Ru(CH_3)I(CO)$_2$(iPr-DAB) (**2a**) (11 mg, 0.03 mmol) and PPh_3 (25.1 mg, 0.1 mmol) were dissolved in 0.5 mL of $CDCl_3$, and the solution was placed in a NMR tube. The reaction was monitored with ^1H and ^{31}P NMR: after 2 h at 20 °C no reaction had taken place; after 2 h at 45 °C circa 10% of [Ru(CH_3)(CO)$_2$(PPh_3)(iPr-DAB)][I] (**8a**) was formed. Selected NMR data for **8a**: ^1H NMR ($CDCl_3$) δ 0.30 (d, J(P—H) = 3.9 Hz, 3H, Ru—C*H*$_3$), 0.89, 1.29 (d, J = 6.5 Hz, 6H, CH(C*H*$_3$)$_2$), 3.80 (sept, J = 6.5 Hz, 2H, C*H*(CH_3)$_2$), 9.19 (d, J(P—H) = 3.0 Hz, 2H, N=C(*H*)); ^{31}P NMR ($CDCl_3$) δ 17.6 (*P*Ph_3).

(iii) At High Temperatures. A suspension of **2a** (225 mg, 0.66 mmol) in 30 mL of heptane was refluxed for 18 h. After evaporation of the solvent complexes **2a** and Ru(CH_3)I(CO)$_2$(CH(CH_3)$_2$N=CHCH_2N=C(CH_3)$_2$) (**11**) were isolated (ratio 4/1). NMR data for **11** agreed with ref 6.

Reactions of Ru(C(O)CH_3)I(CO)$_2$(iPr-DAB) (3a). (i) With Ru(CO)$_4$(PMe_2Ph). A solution of Ru(C(O)CH_3)I(CO)$_2$(iPr-DAB) (**3a**) (8 mg, 0.02 mmol) and Ru(CO)$_4$(PMe_2Ph) (**13**) (7 mg, 0.02 mmol) in 0.5 mL of $CDCl_3$ was placed in an NMR tube. The reaction was monitored with ^1H and ^{31}P NMR: after 2 h at 45 °C **13** was completely converted to **15** while **3a** had not reacted.

(ii) At High Temperatures. A solution of **3a** (7 mg, 0.02 mmol) in 10 mL of heptane was refluxed for 18 h. After evaporation of the solvent NMR revealed the formation of complexes **2a** and Ru(CH_3)I(CO)$_2$(CH(CH_3)$_2$N=CHCH_2N=C(CH_3)$_2$) (**11**) in a three to one ratio. NMR data for **11** agreed with ref 6.

Reactions of [Ru(CH_3)(CO)$_2$(iPr-DAB)][OTf] (4a). (i) With Ru(^{13}CO)$_4$(PMe_2Ph). [Ru(CH_3)(CO)$_2$(iPr-DAB)][OTf] (**4a**) (7 mg, 0.015 mmol) and Ru(^{13}CO)$_4$(PMe_2Ph) (**13**) (7 mg, 0.02 mmol) were dissolved in 0.5 mL of $CDCl_3$, and the solution was placed in an NMR tube. The reaction was monitored with ^1H and ^{31}P NMR and showed the appearance of new signals (minor species 10%, major species **B1** 45%), which disappeared again after 3 h at 20 °C under formation of [Ru(C(O)CH_3)(CO)$_2$(iPr-DAB)][OTf] (**5a**) and **15**. ^{13}C NMR showed that ^{13}CO enrichment had taken place in both carbonyl groups and the acetyl group of **5a**. Spectroscopic data for **B1** [Ru(CH_3)(CO)$_2$(iPr-DAB)-Ru(CO)$_4$(PMe_2Ph)][OTf] are given in Table 5.

(ii) With Ru(CO)$_4$(PMe_2Ph) and Subsequent Addition of PPh_3. [Ru(CH_3)(CO)$_2$(iPr-DAB)][OTf] (**4a**) (13 mg, 0.03 mmol) and Ru(CO)$_4$(PMe_2Ph) (**9**) (10 mg, 0.03 mmol) were dissolved in 0.5 mL of $CDCl_3$, and the solution was placed in an NMR tube. After 10 min at 20 °C PPh_3 (7 mg, 0.03 mmol) was added to the dark red solution of the mixture **4a**, **13**, and **B1**. Within 10 min **B1** and **4a** had disappeared under formation of [Ru-

$(CH_3)(CO)_2(PPh_3)$(iPr-DAB)][OTf] (**9b**) and re-formation of **13**, as revealed by ^1H and ^{31}P NMR.

(iii) With $Ru(CO)_4(PMe_2Ph)$ and Subsequent Addition of NEt_4I. $[Ru(CH_3)(CO)_2$(iPr-DAB)][OTf] (**4a**) (12 mg, 0.03 mmol) and $Ru(CO)_4(PMe_2Ph)$ (**13**) (9 mg, 0.03 mmol) were dissolved in 0.5 mL of $CDCl_3$, and the solution was placed in an NMR tube. After 10 min at 20 °C NEt_4I (5 mg, 0.02 mmol) was added to this mixture of **4a**, **B1**, and **13**, and the solution turned from dark red to dark brown. ^1H and ^{31}P NMR showed the presence of $Ru(CH_3)I(CO)_2$(iPr-DAB) (**2a**) and **13**.

Synthesis of $Ru(CH_3)Cl(CO)_2$(iPr-DAB) (6a). To a yellow solution of $[Ru(CH_3)(CO)_2$(iPr-DAB)][OTf] (**4a**) (56 mg, 0.12 mmol) in 40 mL of dichloromethane was added NEt_4Cl (30 mg, 0.18 mmol). After stirring for 2 h in the dark at 20 °C, the solution turned orange. The solvent was evaporated, and the residue was placed on a column. Elution with THF yielded an orange fraction which contained pure **6a**. (38 mg, yield 95%). IR (CH_2Cl_2): ν(CO) 2030 (s), 1960 (s) cm^{-1}. ^1H NMR ($CDCl_3$): δ −0.21 (s, 3H, Ru−CH_3), 1.52, 1.56 (d, J = 6.6 Hz, 6H, CH(CH_3)$_2$), 4.33 (sept, J = 6.6 Hz, 2H, CH(CH$_3$)$_2$), 8.19 (s, 2H, N=C(H)); ^{13}C NMR ($CDCl_3$): δ −15.8 (Ru−CH_3), 22.9 and 23.1 (CH(CH_3)$_2$), 65.8 (CH(CH$_3$)$_2$), 162.4 (N=CH), 199.0 (CO's).

Reactions of $Ru(CH_3)Cl(CO)_2$(iPr-DAB) (6a). (i) With CO. A solution of **6a** (42 mg, 0.13 mmol) in 15 mL of $CHCl_3$ was refluxed for 20 h under 1 atm of CO (2-L CO vessel). After evaporation of the solvent complex $Ru(C(O)CH_3)Cl(CO)_2$(iPr-DAB) (**7a**) was isolated in 100% yield. NMR data for **7a**: ^1H NMR ($CDCl_3$) δ 1.37, 1.42 (d, J = 6.6 Hz, 6H, CH(CH_3)$_2$), 2.45 (s, 3H, Ru−C(O)CH_3), 4.17 (sept, J = 6.6 Hz, 2H, CH(CH$_3$)$_2$), 8.28 (s, 2H, N=C(H)); ^{13}C NMR ($CDCl_3$) δ 22.6 and 23.0 (CH(CH_3)$_2$), 65.9 (CH(CH$_3$)$_2$), 162.9 (N=CH), 197.0 (CO's), 256.6 (Ru−C(O)CH$_3$).

(ii) With $Ru(CO)_4(PMe_2Ph)$ Under a CO Atmosphere. A solution of **6a** (13 mg, 0.032 mmol) and $Ru(CO)_4(PMe_2Ph)$ (**13**) (6 mg, 0.02 mmol) in 2.5 mL of $CDCl_3$ in a high pressure NMR tube was pressurized with CO (16 atm). The HP NMR tube was brought to 45 °C, and the reaction was monitored with ^1H and ^{31}P NMR. After 2 h all **6a** had disappeared and $Ru(C(O)CH_3)Cl(CO)_2$(iPr-DAB) (**7a**) was formed in quantitative yield, while **13** was still present. No intermediates were observed.

(iii) With $Ru(CO)_4(PMe_2Ph)$ and PPh_3. A solution of **6a** (6 mg, 0.016 mmol), $Ru(CO)_4(PMe_2Ph)$ (**13**) (6 mg, 0.02 mmol), and PPh_3 (4 mg, 0.015 mmol) in 0.5 mL of $CDCl_3$ was placed in an NMR tube. The reaction was monitored with ^1H and ^{31}P NMR: in the beginning of the reaction at 45 °C circa 20% of $[Ru(CH_3)(CO)_2$(iPr-DAB)$(PPh_3)]$[Cl] (**10a**) was formed; after 10 h at 45 °C 50% of **6a** was converted to $Ru(C(O)CH_3)Cl(CO)_2$(iPr-DAB) (**7a**), while **10a** and free PPh_3 had disappeared and **13** was totally converted to **16**.

(iv) With PPh_3. To a solution of **6a** (9 mg, 0.025 mmol) in 0.5 mL of $CDCl_3$ was added at 20 °C PPh_3 (6 mg, 0.03 mmol). Directly, the color of the solution turned from orange to yellow. ^1H and ^{31}P NMR revealed that at 20 °C all **6a** had been converted to $[Ru(CH_3)(CO)_2$(iPr-DAB)$(PPh_3)]$[Cl] (**10a**). NMR data for **10a**; ^1H NMR ($CDCl_3$) δ 0.24 (d, J(P−H) = 3.5 Hz, 3H, Ru−CH_3), 0.71 and 1.27 (d, J = 6.5 Hz, 6 H, CH(CH_3)$_2$), 3.80 (sept, J = 6.5 Hz, 2H, CH(CH$_3$)$_2$), 7.1−7.7 (m, 15 H, C$_6H_5$), 8.69 (s, 2H, N=C(H)); ^{13}C NMR ($CDCl_3$) δ −2.5 (Ru−CH_3), 22.3 and 24.2 (CH(CH_3)$_2$), 64.9 (CH(CH$_3$)$_2$), 129−137 ($C6H_5$), 164.4 (N=CH), 201.1, 201.2 (CO's); ^{31}P NMR ($CDCl_3$) δ 17.1 (PPh_3).

Decarbonylation of $Ru(C(O)CH_3)Cl(CO)_2$(iPr-DAB) (7a). A solution of **7a** (44 mg, 0.12 mmol) in 20 mL of heptane was refluxed for 3 h under 1 atm. After evaporation of the solvent complex $Ru(CH_3)Cl(CO)_2$(iPr-DAB) (**6a**) was isolated in 100% yield.

Reactions of $RuI_2(CO)_2$(iPr-Pyca) (1b). (i) With ^{13}CO. A solution of $RuI_2(CO)_2$(iPr-Pyca) (**1b**) (30 mg, 0.05 mmol) in 1.5 mL of $CDCl_3$ was placed in a closed 10-mm NMR tube and placed under a ^{13}CO atmosphere (1 atm). The reaction was monitored with ^1H and ^{31}P NMR: after 3 days at 45 °C no reaction had taken place.

(ii) With $Ru(^{13}CO)_4(PMe_2Ph)$ (13). A solution of $RuI_2(CO)_2$(iPr-Pyca) (**1b**) (15 mg, 0.026 mmol) and ^{13}CO enriched **13** was refluxed in 25 mL of CH_2Cl_2 for 4 h. After evaporation of the solvent ^{13}C NMR revealed that ^{13}CO was incorporated in **1b**.

Reactions of $Ru(CH_3)I(CO)_2$(iPr-Pyca) (2b). (i) With $Ru(CO)_4(PMe_2Ph)$ and PPh_3. A solution of $Ru(CH_3)I(CO)_2$(iPr-Pyca) (**2b**) (6 mg, 0.014 mmol), $Ru(CO)_4(PMe_2Ph)$ (**13**) (5 mg, 0.014 mmol), and PPh_3 (5 mg, 0.018 mmol) in 0.5 mL of CD_2Cl_2 was placed in an NMR tube. The reaction was monitored with ^1H and ^{31}P NMR: after 20 h at 20 °C no reaction had taken place; after 30 min at 45 °C 30% of **13** was converted to $Ru(CO)_3(PMe_2Ph)(PPh_3)$ (**14**) and no conversion of **2b** was observed.

In $CDCl_3$ (0.5 mL) at 45 °C (**2b** 10 mg, 0.02 mmol; **13** 14 mg, 0.04 mmol; PPh_3 16 mg, 0.06 mmol) after 17 h **2b** was 17% converted to **3b** and 27% converted to $[Ru(CH_3)(CO)_2(PPh_3)$(iPr-Pyca)][I] (**8b**), while **13** was 80% converted to $[Ru(CO)_3(PMe_2Ph)(PPh_3)Cl]_2$ (**16**), as observed by ^1H and ^{31}P NMR.

(ii) With PPh_3. $Ru(CH_3)I(CO)_2$(iPr-Pyca) (**2b**) (12 mg, 0.03 mmol) and PPh_3 (23 mg, 0.1 mmol) were dissolved in 0.5 mL of $CDCl_3$, and the solution was placed in an NMR tube. The reaction was monitored with ^1H and ^{31}P NMR: after 2 h at 20 °C no reaction had taken place; after 2 h at 45 °C circa 40% of $[Ru(CH_3)(CO)_2(PPh_3)$(iPr-Pyca)][I] (**8b**) was formed.

(iii) With $Ru(CO)_4(PMe_2Ph)$. A solution of $Ru(CH_3)I(CO)_2$(iPr-Pyca) (**2b**) (10 mg, 0.02 mmol) and $Ru(CO)_4(PMe_2Ph)$ (**13**) (8 mg, 0.02 mmol) in 0.5 mL of $CDCl_3$ was placed in an NMR tube. The reaction was monitored with ^1H and ^{31}P NMR: after 3 h at 45 °C 16% of **3b** was formed, 11% of an unknown intermediate was formed, and **13** was totally converted to $[Ru(CO)_3(PMe_2Ph)Cl]_2$ (**15**).

Reaction of $[Ru(CH_3)(CO)_2$(iPr-Pyca)][OTf] (4b) with $Ru(^{13}CO)_4(PMe_2Ph)$ (13). $[Ru(CH_3)(CO)_2$(iPr-DAB)][OTf] (**4b**) (5 mg, 0.01 mmol) and $Ru(^{13}CO)_4(PMe_2Ph)$ (**13**) (4 mg, 0.01 mmol) were dissolved in 0.5 mL of $CDCl_3$, and the solution was placed in an NMR tube. The solution turned at 20 °C from yellow to orange. ^1H and ^{31}P NMR showed the formation of a mixture of **4b**, **13**, and $[Ru(CH_3)(CO)_2$(iPr-DAB)$Ru(CO)_4(PMe_2Ph)]$[OTf] (**B2**) (3/3/2) in the beginning of the reaction and quantitative conversion of **4b** to $[Ru(C(O)CH_3)(CO)_2$(iPr-DAB)][OTf] (**5b**) after 2 h at 20 °C. Complex **13** had decomposed into several unknown products. ^{13}C NMR showed that both the carbonyl groups and the acyl group of **5b** were ^{13}CO enriched. Selected spectroscopic data for **B2** are summarized in Table 5.

The same reaction in 10 mL of THF (**4b** 33 mg, 0.07

mmol; **13** 24 mg, 0.07 mmol at 20 °C gave 56% conversion of **4b** to **5b** after 18 h, and 70% conversion after 36 h.

Synthesis of ^{13}CO Enriched $Ru(CO)_4(PMe_2Ph)$ (13). $Ru(^{13}CO)_4(PMe_2Ph)$ (**13**) could be synthesized by stirring $Ru(CO)_4(PMe_2Ph)$ in hexane at 45 °C under 1 atm of ^{13}CO atmosphere.[6] An alternative method is the following: A solution of $Ru_3(CO)_{12}$ (260 mg, 0.40 mmol) in 300 mL of hexane was irradiated under ^{13}CO atmosphere for 8 h (high pressure Hg lamp with Pyrex filter). The ^{13}CO atmosphere was refreshed once, and again the solution was irradiated for 5 h, in which time the solution turned colorless. After this the solution was placed under a nitrogen atmosphere, PMe_2Ph (150 mg, 1.1 mmol) was added, and the solution was stirred for 18 h. The orange solution was reduced in vacuo to 50 mL and placed on a column. Elution with hexane/CH_2Cl_2 (19/1) resulted in a yellow fraction which contained $Ru_3(CO)_{12}$; further elution with hexane/CH_2Cl_2 (40/6) yielded ^{13}CO enriched **13** as a yellow oil (230 mg, yield 55%). IR and NMR data are as reported.[6]

Stability of 13 in hexane, CH_2Cl_2, and THF: stable for 20 h at 20 °C under a N_2 atmosphere; stable for 20 h at 20 °C under a CO atmosphere; stable for 2.5 h at 45 °C under a N_2 atmosphere according to ^{31}P NMR (with IR spectroscopy some unidentified decomposition products can be observed after 2.5 h); stable for 20 h at 45 °C under 1 atm of CO.

Stability of 13 in $CDCl_3$: after 20 h at 20 °C under a N_2 atmosphere complete conversion to **15**; after 20 h at 20 °C under a CO atmosphere complete conversion to **15**; after 2 h at 45 °C under a N_2 atmosphere formation of complex **15**, together with two minor decomposition products (^{31}P NMR of minor products: δ 0.5 and 4.3 ppm in $CDCl_3$); after 3–4 h at 45 °C formation of complex **15** under both 1 and 8 atm of CO pressure; stable for 3 h at 45 °C in $CDCl_3$ in the presence of **2a**, **6a**, and **2b** under 8–16 atm of CO.

Synthesis of $[Ru(CO)_2(PMe_2Ph)Cl]_2$ (15) from 13. A light yellow solution of $Ru(CO)_4(PMe_2Ph)$ (**13**) (80 mg, 0.22 mmol) in 25 mL of $CHCl_3$ was stirred for 18 h at 20 °C, in which time the solution turned bright yellow. After evaporation of the solvent the residue was placed on a column. Elution with hexane/CH_2Cl_2 (2/1) resulted in a yellow fraction which contained a small amount of a not defined ruthenium–phosphine complex. Further elution with hexane/CH_2Cl_2 (20/1) yielded **15** as a bright yellow solid after evaporation of the solvent (58 mg, yield 80%). The same reaction carried out in $CDCl_3$ at 45 °C revealed that **15** was formed in 100% yield after 2.5 h. IR (CH_2Cl_2): ν(CO) 2055 (s), 2026 (vs), 2007 (vs) cm^{-1}. Mass calcd for $C_{20}H_{22}O_4P_2Cl_2Ru$: 662. Found: *m/e* 662. ^1H NMR ($CDCl_3$): δ 2.07 (m, 6H, $P(CH_3)_2$), 7.3–7.8 (m, 5H, PPh). ^{31}P NMR ($CDCl_3$): δ −5.5 (s, PMe_2Ph).

Formation of $[Ru(CO)_2(PMe_2Ph)(PPh_3)Cl]_2$ (16) from 13. A light yellow solution of $Ru(CO)_4(PMe_2Ph)$ (**13**) (80 mg, 0.22 mmol) and PPh_3 (63 mg, 0.24 mmol) in 50 mL of $CHCl_3$ was stirred for 24 h at 20 °C, in which time the solution turned colorless. After evaporation of the solvent the residue was placed on a column. Elution with hexane/CH_2Cl_2 (2/1) and later CH_2Cl_2 resulted in a few orange fractions which contained very small amounts of not defined ruthenium complexes. Further elution with CH_2Cl_2/diethyl ether (20/1) yielded a light yellow solution, which resulted in an almost colorless solid after evaporation of the solvent (100 mg, yield 84%). IR (CH_2Cl_2): ν(CO) 2053 (s), 1991 (vs) cm^{-1}. Mass calcd for $C_{56}H_{52}O_4P_4Cl_2Ru_2$; 1186. Found: *m/e* 593. ^1H NMR (acetone-d_6): δ 2.22 (dd, ^2J(P–H) = 11.1 and ^4J(P–H) = 2.1 Hz) 6 H, $P(CH_3)_2$), 7.5–8.2 (m, 5H, PPh). ^{13}C NMR (acetone-d_6): δ 12.7 (d, J(P–C) = 35.3 Hz, PMe), 129.3/129.8/130.8/131.5/131.7/135.2 (phenyl carbon atoms), 133.7 (dd, J(P–C) = 42.3/3.0 Hz, Ph C1 of PPh_3), 137.0 (dd, J(P–C) = 44.5/3.0 Hz, Ph C1 of PMe_2Ph), 194.0 (dd, J(P–C) = 11.3/9.8 Hz, CO). ^{31}P NMR (acetone-d_6): δ 5.2 (d, J(P–P) 343 Hz, PMe_2Ph), 16.6 (d, J(P–P) = 343 Hz, PPh_3).

Formation of $Ru(CO)_3(PMe_2Ph)(PPh_3)$ (14) from 13. A light yellow solution of $Ru(CO)_4(PMe_2Ph)$ (**13**) (6 mg, 0.02 mmol) and PPh_3 (4 mg, 0.02 mmol) in 20 mL of THF was stirred for 2 h at 45 °C. After evaporation of the solvent **14** was isolated in quantitative yield. IR and NMR data agree with those reported.[6]

X-ray Structure Determination of 4b. A crystal with dimensions 0.10 × 0.10 × 0.80 mm approximately was used for data collection on an Enraf-Nonius CAD-4 diffractometer with Cu Kα radiation and the ω–2θ scan. A total of 3575 unique reflections were measured within the range $0 < h < 10$, $0 < k < 14$, $-22 < l < 21$. Of these, 3075 were above the significance level of 2.5$\sigma(I)$. The maximum value of $(\sin\Theta)/\lambda$ was 0.61 Å^{-1}. Two reference reflections (021, 1,1,−4) were measured hourly and showed no decrease during the 40-h collecting time. Unit-cell parameters were refined by a least-squares fitting procedure using 23 reflections with $80 < 2\Theta < 85°$. Corrections for Lorenz and polarization effects were applied. The position of Ru was found by direct methods. The remainder of the non-hydrogen atoms were found in a subsequent ΔF synthesis. The hydrogen atoms were calculated. Full-matrix least-squares refinement of F, anisotropic for the non-hydrogen atoms and isotropic for the hydrogen atoms, restraining the latter in such a way that the distance to their carrier remained constant at approximately 1.09 Å, converged to $R = 0.037$, $R_w = 0.052$, and $(\Delta/\sigma)_{max} = 0.60$. A weighing scheme $w = (6.7 + F_o + 0.0066F_o^2)^{-1}$ was used. An empirical absorption correction (DIFABS)[13] was applied, with coefficients in the range 0.76–1.28. Scattering factors were taken from Cromer and Mann.[14] The anomalous scattering of Ru and S was taken into account. All calculations were performed with XTAL.[15] A view[16] of the structure and the atomic numbering is shown in Figure 2. Crystallographic data and fractional coordinates are collected in Tables 1 and 2, respectively.

Results and Discussion

The discussion is split in three major parts. Firstly, the synthesis of the new complexes $Ru(R)X(CO)_2(R'$-Pyca) (R = I, CH_3, $C(O)CH_3$; X = I, OTf; R′ = $CH_3OCH_2CH_2$ and $iPrOCH_2CH_2CH_2$) will be presented. Secondly, the results of additional experiments to clarify the reaction mechanism of the $Ru(CO)_4(PMe_2Ph)$ (**13**) assisted CO insertion of $Ru(CH_3)X(CO)_2$(iPr-DAB) (X = I

(13) Walker, N.; Stuart, D. *Acta Crystallogr.* **1983**, *A39*, 158.
(14) Cromer, D. T.; Mann, J. B. *Acta Crystallogr.* **1968**, *A24*, 321. *International Tables for X-ray Crystallography*; Kynoch Press: Birmingham, U.K., 1974; Vol. 4, p 55.
(15) Hall, S. R., Steward, J. M., Eds. *XTAL3.0* User's Manual. Universities of Western Australia and Maryland, 1990.
(16) Motherwell, W. D. S.; Clegg, W. **1978**, *PLUTO*, Program for plotting molecular and crystal structures. University of Cambridge, 1978.

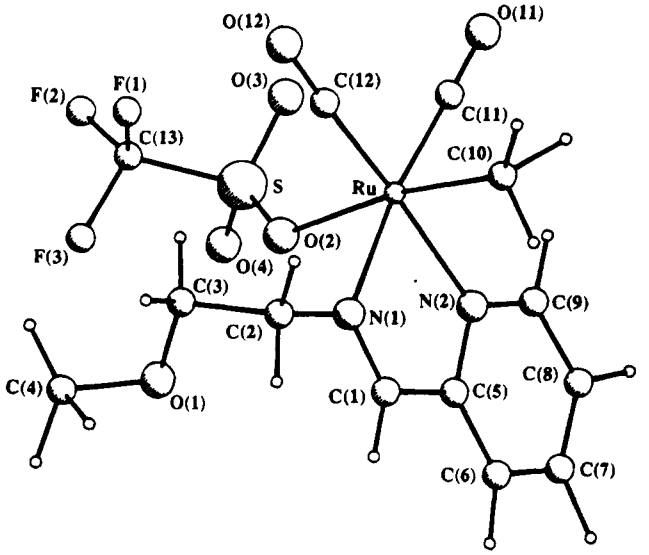

Figure 2. X-ray structure of [Ru(CH$_3$)(CO)$_2$(CH$_3$OCH$_2$-CH$_2$-Pyca)][OTf] (**4c**).

Table 1. Crystallographic Data for [Ru(CH$_3$)(CO)$_2$(CH$_3$OCH$_2$CH$_2$-Pyca)][OTf] (4c)

formula	$C_{13}H_{15}N_2O_6SF_3Ru$	V (Å^3)	1893.4(2)
mol wt	485.4	Z	4
cryst syst	monoclinic	T (K)	293
space group	$P2_1/c$	D_{calc} (g/cm^{-1})	1.7
a (Å)	8.5008(4)	λ(Cu Kα) (Å)	1.5418
b (Å)	12.3281(8)	μ(Cu Kα) (cm^{-1})	84.5
c (Å)	18.412(1)	(sin θ)/λ (Å^{-1})	0.61
β (deg)	101.118(6)	no. of data collected	3575
F(000)	968	final R for 3075 obs refl	0.037

Table 2. Final Atomic Coordinates and Equivalent Isotropic Thermal Parameters for [Ru(CH$_3$)(CO)$_2$(CH$_3$OCH$_2$CH$_2$-Pyca)][OTf] (4c) (Esds in Parentheses)

	x	y	z	U_{eq} (Å^3)
Ru	0.26095(4)	0.29428(2)	0.46611(2)	0.0507(2)
S	0.04048(1)	0.0931(1)	0.37245(7)	0.0651(6)
C(1)	−0.0718(5)	0.2317(4)	0.4555(2)	0.059(2)
C(2)	−0.0737(7)	0.3587(5)	0.3599(3)	0.078(3)
C(3)	−0.0467(8)	0.3152(5)	0.2879(3)	0.083(4)
C(4)	−0.133(2)	0.173(1)	0.2054(5)	0.159(9)
C(5)	0.0089(5)	0.1682(4)	0.5184(2)	0.055(2)
C(6)	−0.0713(6)	0.0976(4)	0.5567(3)	0.069(3)
C(7)	0.0153(7)	0.0388(4)	0.6144(3)	0.073(3)
C(8)	0.1777(7)	0.0515(4)	0.6323(3)	0.077(3)
C(9)	0.2520(6)	0.1246(4)	0.5921(3)	0.066(3)
C(10)	0.2204(7)	0.4203(5)	0.5368(3)	0.081(4)
C(11)	0.4748(6)	0.2920(4)	0.5148(3)	0.070(3)
C(12)	0.3212(7)	0.3960(4)	0.4026(3)	0.080(3)
C(13)	0.388(1)	0.130(1)	0.2769(4)	0.132(7)
N(1)	0.0100(4)	0.2935(3)	0.4232(2)	0.055(2)
N(2)	0.1697(4)	0.1818(3)	0.5357(2)	0.052(2)
O(1)	−0.1117(6)	0.2105(4)	0.2778(2)	0.099(3)
O(2)	0.2689(3)	0.1496(3)	0.3929(2)	0.065(2)
O(3)	0.5567(4)	0.1323(4)	0.4066(2)	0.100(3)
O(4)	0.3845(6)	−0.0218(3)	0.3688(3)	0.144(4)
O(11)	0.6050(5)	0.2964(4)	0.5444(3)	0.104(3)
O(12)	0.3612(7)	0.4598(4)	0.3656(3)	0.132(4)
F(1)	0.384(1)	0.2291(7)	0.2654(4)	0.228(8)
F(2)	0.4986(7)	0.0833(7)	0.2476(3)	0.191(5)
F(3)	0.2427(9)	0.0907(8)	0.2396(3)	0.207(7)

(**2a**), OTf (**4a**), Cl (**6a**)) will be discussed, and the acylation reactions of **2a** and **4a** will be compared with those of complexes Ru(CH$_3$)X(CO)$_2$(iPr-Pyca) (X = I (**2b**), OTf (**4b**)). In the reactions of **2b**, **4a**, and **4b** with Ru(CO)$_4$(PMe$_2$Ph) (**13**), complex **13** decomposed. The stability of **13** under different reaction conditions and the decomposition products of **13** will be treated in the last section.

Synthesis of Ru(R)X(CO)$_2$(α-diimine) (R = I, X = I (1); R = CH$_3$, X = I (2); R = acyl, X = I (3); R = CH$_3$, X = OTf (4); R = acyl, X = OTf (5); R = CH$_3$, X = Cl (6); R = acyl, X = Cl (7)). In Scheme 2 the synthetic routes to the Ru(R)X(CO)$_2$(α-diimine) complexes are shown. Full data for all new complexes are reported in the Experimental Section. Complexes **1a**–**5a** with the iPr-DAB ligand and **1b** and **2b** have been described before.[6]

Starting from [Ru(CO)$_3$(R′-Pyca)], which is in situ prepared from Ru$_3$(CO)$_{12}$ and excess R′-Pyca,[10] addition of MeI yields RuI$_2$(CO)$_2$(R′-Pyca) (**1**: 10%), Ru(CH$_3$)I(CO)$_2$(R′-Pyca) (**2**: 75–80%), and Ru(C(O)CH$_3$)I(CO)$_2$(R′-Pyca) (**3**: 10–15%) (R′ = iPr (**b**); R′ = methoxyethyl (**c**); R′ = isopropoxypropyl (**d**)), respectively. Complex **1** could also be synthesized but in quantitative yield by addition of I$_2$ to [Ru(CO)$_3$(α-diimine)] (Scheme 2).[10] The methyl complexes **2c** and **2d** have spectroscopic properties similar to those of Ru(CH$_3$)I(CO)$_2$(iPr-Pyca) (**2b**). The carbonyl stretches are observed at 2029 and 1965 (**2c**) and 2030 and 1963 (**2d**) cm^{-1} in the IR. Because complexes **2b**, **2c**, and **2d** are asymmetric, two signals are observed for the carbonyl groups in the ^{13}C NMR (circa 202 ppm for **2b**, **2c**, and **2d**). The methyl group resonates at 0.04 ppm for both **2c** and **2d** (^{1}H NMR) and at −5.4 (**2c**) and −5.2 (**2d**) ppm (^{13}C NMR), respectively.

In addition to complexes **1** and **2**, also 10–15% of Ru(C(O)CH$_3$)I(CO)$_2$(R′-Pyca) (**3**) was isolated, as already mentioned.[10b] Complexes **3b**, **3c**, and **3d** all show carbonyl stretches at 2040 and 1980 cm^{-1}. In solution no signal of the acyl moiety (expected at circa 1720 cm^{-1}) could be observed, because this signal was too weak. In the NMR spectra the acyl group shows a singlet at about 2.45–2.51 ppm for **3b**, **3c**, and **3d** (^{1}H NMR). The ^{13}C NMR spectra show the acyl group on the metal at circa 49 ppm (C(O)*C*H$_3$) and at circa 240 ppm (*C*(O)CH$_3$) for **3b**, **3c**, and **3d**. The carbonyl ligands of **3b**, **3c**, and **3d** appear at about 199–200 ppm in the ^{13}C NMR spectra. These data clearly indicate that complexes **3b**, **3c**, and **3d**, with different R′-Pyca ligands, do not differ much in spectroscopic properties, indicating very similar structures in solution.

The ionic complexes [Ru(CH$_3$)(CO)$_2$(R′-Pyca)][OTf] (**4b** and **4c**) were synthesized by addition of AgOTf to Ru(CH$_3$)I(CO)$_2$(R′-Pyca) (**2b** and **2c**, respectively) (Scheme 2). For complexes containing ligand **d** no ionic complexes could be isolated, due to decomposition of the products. The IR spectra of **4b** and **4c** show the carbonyl vibrations at 2040 and 1975 cm^{-1} (**4b**) and at 2040 and 1965 (**4c**) cm^{-1}, respectively. The CO resonances of the carbonyl ligands in ^{13}C NMR have shifted from circa 202 for the neutral complexes **2** to 199 ppm for the ionic species **4**. Both IR and NMR indicate a decreased π-back-bonding in going from the neutral complexes **2** to the ionic complexes **4**, as expected because of the more electron poor ruthenium center in the latter complexes.

For complex **4c** the X-ray structure shows the coordination of the triflate group trans to the methyl group in the solid state (vide infra). The IR (KBr) spectrum of **4c** confirms that the triflate is coordinated, as $\nu_{as}(SO_3)$ is observed at 1318 (s) cm^{-1}, whereas $\nu_{as}(SO_3)$ for ionic OTf is found at 1280 cm^{-1}.[17] From IR and NMR data

(17) (a) Johnston, D. H.; Shriver, D. F. *Inorg. Chem.* **1993**, *32*, 1045. (b) Lawrence, G. A. *Chem. Rev.* **1986**, *86*, 17.

Scheme 2. Synthesis of Complexes Ru(R)X(CO)$_2$(α-diimine) with Ligands a–d

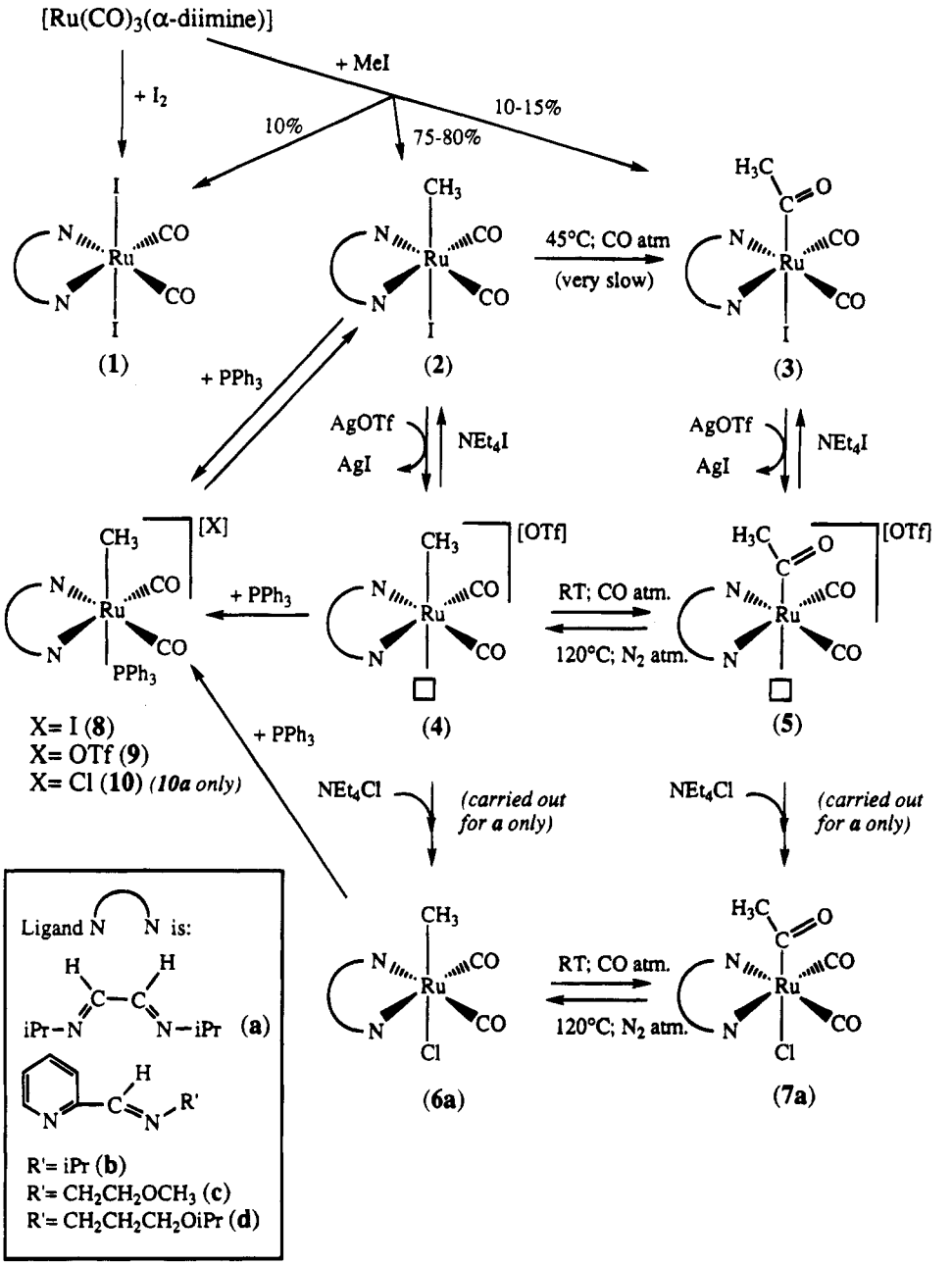

it could not be deduced whether the triflate remains coordinated in solution or not. The data do not suggest an intra- or intermolecular coordination of the ether arm either. Molecular models (CPK) suggest that the ether arm is flexible enough and that there is enough space for an oxygen–ruthenium interaction. Significant shifts of the protons of the ether arm are expected upon coordination of the ether oxygen atom to the metal, i.e. upon closing of the ether arm.[18] However, if a fast equilibrium exists between a small amount of complex in which the ether arm is coordinated and a complex in which the ether arm is not coordinated, the ^{1}H NMR spectra will not be affected visibly.

Stirring of **4** under CO atmosphere at 20 °C yielded complex [Ru(C(O)CH$_3$)(CO)$_2$(R'-Pyca)][OTf] (**5**) within 15 min, in which CO insertion has taken place (Scheme 2). As was reported for **5a**, the vacant site in **5b** and **5c** is not occupied by CO at 1 atm.[6] In solution there is most probably a fast equilibrium between coordinating and not coordinating triflate at the open site, similar to complexes **4**. The NMR spectra of complexes **4** and **5** do not show significant differences, indicating that the influence of the acyl group in the ionic complex does not differ much from that of the methyl group, which is understandable, since in compounds **4** and **5** there is in principle an open coordination site trans to the methyl and acyl groups, respectively.

By addition of NEt$_4$Cl to [Ru(CH$_3$)(CO)$_2$(iPr-DAB)][OTf] (**4a**) complex Ru(CH$_3$)Cl(CO)$_2$(iPr-DAB) (**6a**) was produced. The spectroscopic data for **2a** and **6a** (NMR and IR) are very similar. Only the resonance of the methyl group in **6a** is shifted to lower field compared to **2a** (^{1}H NMR: δ −0.04 and −0.21 ppm, respectively). This means that the methyl group in **6a** is somewhat more shielded than in **2a**. The synthesis of complexes [Ru(CH$_3$)(CO)$_2$(α-diimine)(PPh$_3$)][X] with X = I (**8**), X = OTf (**9**), and X = Cl (for iPr-DAB only: **10a**) was carried out because of the presence of these complexes

(18) Unpublished ^{1}H NMR data for [CpRu(Ph$_2$PCH$_2$CH$_2$OCH$_3$)$_2$][SbF$_6$].[19]

Table 3. Selected Bond Distances (Å) and Angles (deg) for [Ru(CH$_3$)(CO)$_2$(CH$_3$OCH$_2$CH$_2$-Pyca)][OTf] (4c) (Esds in Parentheses)

Ru–C(10)	2.098(6)	C(1)–C(5)	1.456(6)
Ru–C(11)	1.866(5)	C(1)–N(1)	1.256(6)
Ru–C(12)	1.853(6)	C(2)–C(3)	1.489(8)
Ru–N(1)	2.127(4)	C(2)–N(1)	1.480(6)
Ru–N(2)	2.133(4)	C(3)–O(1)	1.403(8)
Ru–O(2)	2.245(3)	C(4)–O(1)	1.39(1)
S–C(13)	1.794(9)	C(5)–N(2)	1.353(5)
S–O(2)	1.459(3)	C(11)–O(11)	1.136(7)
S–O(3)	1.408(4)	C(12)–O(12)	1.135(9)
S–O(4)	1.426(4)		
C(10)–Ru–O(2)	171.4(2)	C(13)–S–O(3)	104.2(4)
C(11)–Ru–O(2)	97.9(2)	C(13)–S–O(4)	102.6(5)
C(12)–Ru–O(2)	96.6(2)	C(5)–C(1)–N(1)	119.0(4)
N(1)–Ru–N(2)	76.4(1)	C(1)–C(5)–N(2)	114.8(4)
N(1)–Ru–O(2)	85.3(1)	C(3)–O(1)–C(4)	114.1(7)
N(2)–Ru–O(2)	84.3(1)	Ru–O(2)–S	130.6(2)
C(13)–S–O(2)	102.3(4)		

during the stoichiometric acylation reactions of complexes **2**, **4**, and **6** with **13** and PPh_3 (vide infra). Whereas complexes **2** and **8** are in equilibrium with each other at 45 °C (ratio **2/8** = 55/45), addition of PPh_3 to **4a** or **6a** at 20 °C yielded complexes **9a** and **10a** in quantitative yield. The spectroscopic data for **8a**, **8b**, **9a**, **9b**, and **10a** are very similar, as expected.

Addition of PPh_3 to [Ru(acyl)(CO)$_2$(iPr-DAB)][OTf] (**5b**) yielded [Ru(acyl)(CO)$_2$(iPr-DAB)(PPh_3)][OTf] in quantitative yield (not in Scheme 2). The NMR signal of the triphenylphosphine ligand appeared at 18.2 ppm in the ^{31}P NMR spectrum.

X-ray Structure of [Ru(CH$_3$)(CO)$_2$(CH$_3$OCH$_2$CH$_2$-Pyca)][OTf] (4c). In Figure 2 the molecular structure of **4c** is shown together with the atom numbering. Selected bond distances and angles of **4c** are listed in Table 3. The molecule consists of a ruthenium center which is octahedrally coordinated by two carbonyl ligands, two nitrogen atoms, a carbon atom of the methyl group, and an oxygen atom of the triflate group trans to each other. The structure is similar to that reported for [Ru(C(O)CH$_3$)(CO)$_2$(iPr-DAB)][OTf] (**5a**),[6] which has the triflate group coordinated trans to the acyl moiety.

The C(1)–N(1) (1.256(6) Å) and C(1)–C(5) (1.456(6) Å) bond distances are only slightly longer, and shorter, respectively, than reported for free cyclohexyl–DAB (cHex-DAB: 1.258(3) and 1.457(3) Å, respectively).[20] As in the case of Ru(CH$_3$)I(CO)$_2$(iPr-DAB) (**2a**)[6] and [Ru(C(O)CH$_3$)(CO)$_2$(iPr-DAB)][OTf] (**5a**),[6] this points to only limited π-back-bonding from the electron poor ruthenium center to the α-diimine.

The bond distances of the ruthenium–methyl bond (Ru–C(10): 2.098(6) Å) and the Ru–O(2) bond (2.345(3) Å) and the distances within the triflate molecule in **4c** are similar to those of **5a** (for **5a**: Ru–C(acyl) = 2.122(9) and Ru–O(2) = 2.239(5) Å, respectively).[6] The bond angles Ru–O(2)–S, C(13)–S–O(2), C(13)–S–O(3), and C(13)–S–O(4) in **4c** (see Table 3) are equal to those of **5a** (for **5a**: 130.5(3), 102.7(5), 104.0(5), and 103.0(6)°, respectively), whereas the C(10)–Ru–O(2) angles of 171.4(2)° in **4c** is somewhat larger than that in **5a** (168.2(3)°).[6] Apparently, the replacement of the iPr-DAB ligand by CH$_3$OCH$_2$CH$_2$-Pyca does lead to only very small changes in the structural features of [Ru(R)(CO)$_2$(α-diimine)][OTf].

The methoxyethyl arm on the ligand in **4c** is bent away from the metal center and does not interact with the metal, in contrast to similar Ru(II) complexes containing ether–phosphine ligands, such as RuCl$_2$(η^2-PPh$_2$CH$_2$CH$_2$OCH$_3$)$_2$[21] and [CpRu(η^2-PPh$_2$CH$_2$CH$_2$OCH$_3$)(PPh$_2$CH$_2$CH$_2$OCH$_3$)][SbF$_6$].[19] In the latter cases the ether arm of the ligand coordinates to the metal center both in the solid state and in solution. Although the coordination of the ether oxygen is rather weak, as may be deduced from the fluxional character, the ruthenium ether–phosphine complexes prefer this coordination above an empty site. Possibly, the strong trans influence of the methyl group of **4c** causes the ether arm not to coordinate. The fact that carbon monoxide only coordinates to the site trans to the methyl group at high pressures in complexes **4**, and not at 1 atm of CO, also confirms the large trans influence of the methyl group.[22] It should be mentioned, however, that in the ruthenium ether–phosphine complexes mentioned above no alternative ligand such as the triflate anion was present to compete with the ether oxygen.

Ru(CO)$_4$(PMe$_2$Ph) Assisted CO Insertion in Ru(CH$_3$)X(CO)$_2$(iPr-DAB) (X = I (2a), OTf (4a), and Cl (6a)). It has been reported that complex Ru(CH$_3$)I(CO)$_2$(iPr-DAB) (**2a**) does not react with CO at low pressures at 45 °C, whereas use of high pressures (8–16 atm) led to conversion of only 20–35%, respectively, after 17 h at 45 °C (Table 4).[6] When Ru(CO)$_4$(PMe$_2$Ph) (**13**) was added to **2a** in the presence of L = CO or PPh_3, a remarkable increase in the acylation rate was observed at 45 °C (Table 4).[6] During this reaction complex Ru(CO)$_4$(PMe$_2$Ph) (**13**) is converted to Ru(CO)$_3$(L)(PMe$_2$Ph) (L = CO (**13**); L = PPh_3 (**14**)). The reaction of **2a** and Ru(^{13}CO)$_4$(PMe$_2$Ph) with CO or PPh_3 at 45 °C resulted in the incorporation of ^{13}CO in both the terminal carbonyl positions and in the acetyl group of **3a**.[6] These results were explained by assuming the presence of the bimetallic intermediate **X1** (see Scheme 1), via which intermolecular carbonyl scrambling between Ru(CH$_3$)I(CO)$_2$(iPr-DAB) (**2a**) and Ru(CO)$_4$(PMe$_2$Ph) (**13**) may take place before acylation occurs.[6]

An alternative rationalization for the ^{13}CO scrambling between **2a** and **13** could be that CO scrambling takes place via an intramolecular acylation process forming **A1**, and subsequent reaction of the acyl intermediate **A1** and **13** to form **A2** (Scheme 3). **A2** differs from intermediate **X1** in Scheme 1 since in **A2** acylation has already taken place. If this was the case we would expect no CO scrambling if RuI$_2$(CO)$_2$(iPr-DAB) (**1a**) is used instead of **2a**. However, although no reaction was observed between RuI$_2$(CO)$_2$(iPr-DAB) (**1a**) and Ru(^{13}CO)$_4$(PMe$_2$Ph) (**13**) in CDCl$_3$ at 20 °C, ^{13}CO was introduced in **1a** at 45 °C, indicating that CO scrambling takes place via a binuclear intermediate, which occurs before the methyl migration step, as proposed in Scheme

(19) de Klerk-Engels, B.; Groen, J. H.; Vrieze, K.; Möckel, A.; Lindner, E.; Goubitz, K.; *Inorg. Chim. Acta* **1992**, *195*, 237.

(20) Keijsper, J.; van der Poel, H.; Polm, L. H.; van Koten, G.; Seignette, P. F. A. B.; Varenhorst, R.; Stam, C. J.; Vrieze, K. *Polyhedron* **1983**, *2*, 1111.

(21) (a) McCann, G. M.; Carvill, A.; Lindner, E.; Karle, B.; Mayer, H. A. *J. Chem. Soc., Dalton Trans.* **1990**, 3107. (b) Bader, A.; Lindner, E. *Coord. Chem. Rev.* **1991**, *108*, 27.

(22) (a) Cardaci, G.; Reichenbach, G.; Bellachioma, G.; Wassink, B.; Baird, M. C. *Organometallics* **1988**, *7*, 2475. (b) Appleton, T. G.; Clark, H. C.; Manzer, L. E. *Coord. Chem. Rev.* **1973**, *10*, 335. (c) Cotton, F. A.; Wilkinson, F. R. S. *Advances in Inorganic Chemistry*, 3rd ed.; Interscience Publishers; New York, 1972; p 667.

Table 4. Summary of the Reactions of $Ru(CH_3)X(CO)_2(\alpha\text{-diimine})$ in $CDCl_3$ (α-diimine = iPr-DAB (a) and X = I (2), X = OTf (4), X = Cl (6); α-diimine = iPr-Pyca (b) and X = I (2), X = OTf (4))

complex	added	intermediate obsd (amt (%))	atmosphere (pressure (atm))	T (°C)	t (h)	(conversion product (%))	fate of 13, if used (amt (%))
2a		none	CO (8−16)	45	17	**3a** (20−35)	
	13	none	CO (8−16)	45	2.5	**3a** (100)	**13**
	13	none	N_2	45	5	**11/12** (1−5)	not known
	13 + PPh_3	**8a**	N_2	45	18	**3a** (100)	**14**
	PPh_3		N_2	45	3	**8a** (45)	
4a		none	CO (1)	20	0.1	**5a** (100)	
	13	**B1** (45%)	N_2	20	0.1		
	13	**B1** (45%)	N_2	20	3	**5a** (100)	**15** (100)
	PPh_3	none	N_2	20	0.1	**9a** (100)	
6a		none	CO (1)	45	18	**7a** (100)	
	13	none	CO (8−16)	45	2	**7a** (100)	
	13	**B**-type	N_2	20	0.1		
	13 + PPh_3	**10a**	N_2	45	10	**7a** (55)	**16** (100)
	PPh_3		N_2	20	0.1	**10a** (100)	
2b		none	CO (16)	45	16	**3b** (40)	
	13	none	CO (12)	45	3.5	**3b** (90)	**13/15** (9/1)
	13	none	N_2	45	3	**3b** (16)	**15** (100)
	13 + PPh_3	**8b**	N_2	45	17	**3b** (17), **8b** (27)	**16** (100)
	PPh_3		N_2	45	4	**8b** (10)	
4b		none	CO (1)	20	0.1	**5b** (100)	
	13	**B2** (45)	N_2	20	0.1		
	13	**B2** (45)	N_2	20	3	**5b** (100)	**15**
	PPh_3		N_2	20	0.1	**9b** (100)	

Scheme 3. ^{13}CO Scrambling in the Reaction of $Ru(CH_3)I(CO)_2(\alpha\text{-diimine})$ (2) with $Ru(CO)_4(PMe_2Ph)$ (13) via Preliminary Acyl Formation

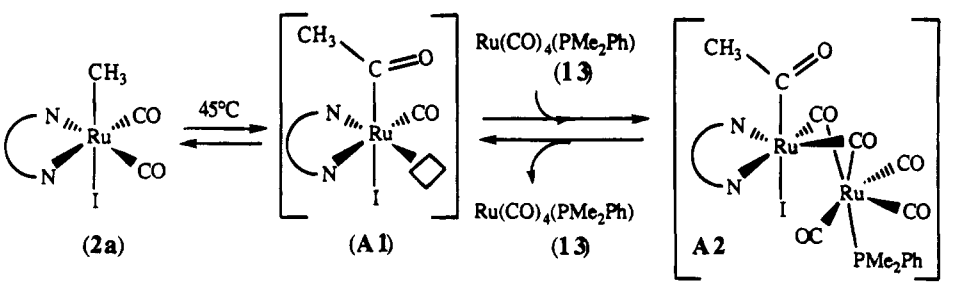

1. Intermediate **X1** must be a very short living species, as no evidence for an intermediate complex with bridging CO's was obtained by ^{13}C NMR and IR spectroscopy.

In this respect it is noteworthy to remark that during the reaction of **2a**, **13**, and PPh_3 at 45 °C in $CDCl_3$, resulting in the formation of $Ru(C(O)CH_3)I(CO)_2$(iPr-DAB) (**3a**) and $Ru(CO)_3(PMe_2Ph)(PPh_3)$ (**14**) within 18 h (Scheme 1), the signals of two species were observed, which disappeared again at the end of the reaction.[6] We tried to identify these species by carrying out stoichiometric reactions of **2a** with $Ru(CO)_4(PMe_2Ph)$ (**13**) in the presence and absence of PPh_3, while at the same time changing the solvent and temperature.

When THF was used instead of $CDCl_3$ in the reaction of **2a**, **13**, and PPh_3 at 45 °C, complex **13** was totally converted to $Ru(CO)_3(PMe_2Ph)(PPh_3)$ (**14**) within 2 h, while only 5% of $Ru(C(O)CH_3)I(CO)_2$(iPr-DAB) (**3a**) was formed. As the formation of **14** from **13** and PPh_3 is much faster in THF (2 h) than in $CDCl_3$ (18 h) and as **14** is not active as an acylation catalyst,[6] the low rate of acylation of **2a** is understandable.

At 20 °C, the reaction of **2a**, **13**, and PPh_3 in $CDCl_3$ did not result in the formation of any product or intermediate. Stirring of **2a** and PPh_3 at 20 °C in the absence of $Ru(CO)_4(PMe_2Ph)$ (**13**) in $CDCl_3$ did not give any reaction, while stirring of **2a** and PPh_3 at 45 °C resulted in the formation of $[Ru(CH_3)(CO)_2(PPh_3)$(iPr-DAB)][I] (**8a**) in 45% yield. Comparison of the spectra data of **8a** with those of the reaction mixture of **2a**, **13**, and PPh_3 showed that the main intermediate species observed in the latter reaction is complex **8a** (Table 4). As it has been proven by Kraakman et al. that the analogous complex $[Ru(CH_3)(CO)_2(PMe_2Ph)$(iPr-DAB)][OTf] could not be acylated,[6] **8a** most probably is a side product in the reaction of **2a**, **13**, and PPh_3, and not an intermediate on the route to the acylated product. Since **8a** is in equilibrium with **2a**, complex **8a** disappears again at the end of the acylation reaction, when all **2a** is converted to **3a** (Scheme 4).

The facile formation of **8a** shows that the iodide in $Ru(CH_3)I(CO)_2$(iPr-DAB) (**2a**) easily dissociates. In connection with this it is worthwhile to note that CO insertion in the case of $Fe(CH_3)I(CO)_2(PMe_2Ph)_2$ took place via an ionic intermediate formed by iodide dissociation in dichloromethane.[22,23] It has further been observed before the $[Ru(CH_3)(CO)_2$(iPr-DAB)][OTf] (**4a**) readily inserts CO at 20 °C to form $[Ru(C(O)CH_3)(CO)_2$(iPr-DAB)][OTf] (**5a**).[6] Therefore, we decided to study whether ionic intermediates might still play a role in the $Ru(CO)_4(PMe_2Ph)$ assisted acylation of **2a**.

Addition of $Ru(^{13}CO)_4(PMe_2Ph)$ (**13**) to $[Ru(CH_3)(CO)_2$(iPr-DAB)][OTf] (**4a**) in $CDCl_3$ at 20 °C resulted in the quantitative formation of $[Ru(C(O)CH_3)(CO)_2$(iPr-DAB)][OTf] (**5a**) within 3 h, while **13** was unexpectedly converted to $[Ru(CO)_3(PMe_2Ph)Cl]_2$ (**15**) (Scheme 5; Table 4). Product **5a** showed ^{13}CO enrichment in both the terminal carbonyl groups and the acyl group, which suggests an equilibrium between **4a** and **13** via a

(23) Bellachioma, G.; Cardaci, G.; Jablonski, C.; Macchioni, A.; Reichenbach, G. *Inorg. Chem.* **1993**, *32*, 2404.

Scheme 4. Reactions of Ru(CH₃)I(CO)₂(iPr-DAB) (2a) with Ru(CO)₄(PMe₂Ph) (13) and PPh₃

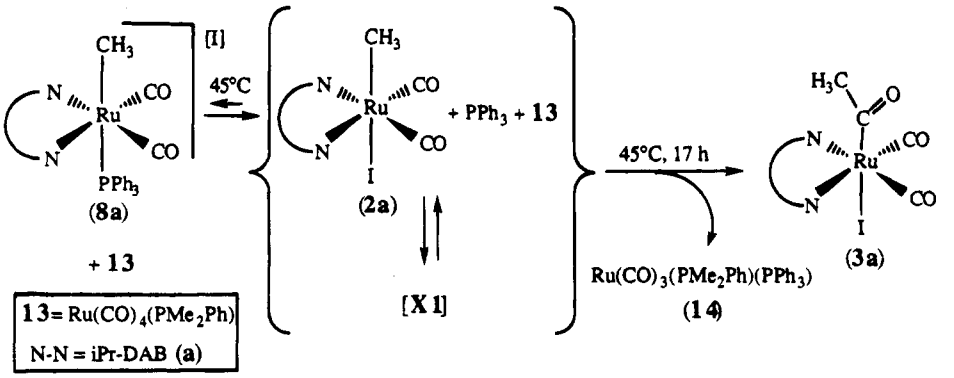

Scheme 5. Reactions of [Ru(CH₃)(CO)₂(iPr-DAB)][OTf] (4a) and Ru(CO)₄(PMe₂Ph) (13) with PPh₃ and NEt₄I

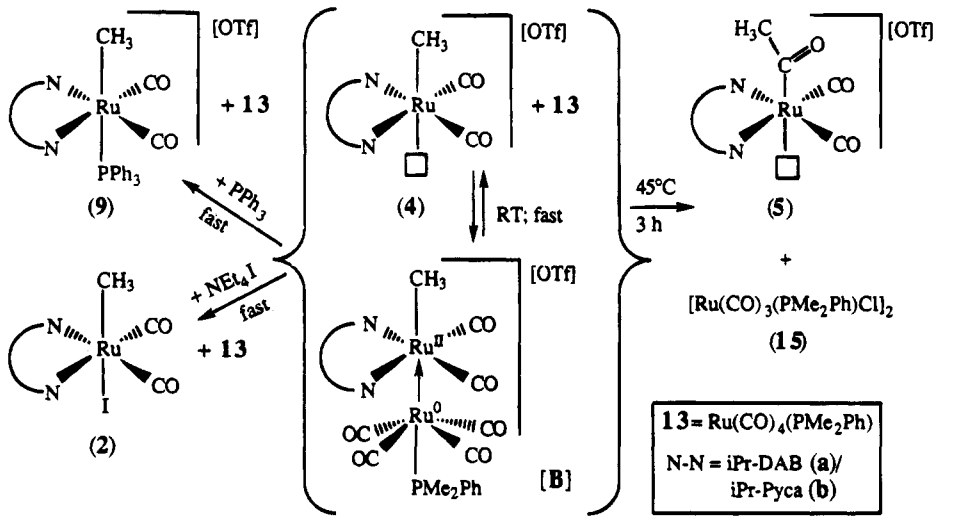

Table 5. Selected Spectroscopic Data of the Intermediates [Ru(CH₃)(CO)₂(α-diimine)Ru(CO)₄(PMe₂Ph)][OTf] (α-diimine = iPr-DAB (B1), iPr-Pyca (B2))

B1	^{1}H NMR, δ (ppm)[a]	0.34 (s, 3H, Ru—CH₃), 2.22 (d, *J*(P—H) = 9.9 Hz, 6H, P—CH₃), 4.44 (sept, *J* = 6.6 Hz, 2H, C*H*(CH₃)₂), 8.49 (s, 2H, N=CH)
	^{13}C NMR, δ (ppm)[a]	198.2 (s), 201.5 (d, *J*(P—C) = 6.8 Hz), 204.5 (s), carbonyl carbon atoms[b]
	^{31}P NMR, δ (ppm)[a]	−8.8 (*P*Me₂Ph)
	IR, ν(CO) (cm^{-1})[c]	1963 (s), 2029 (s), 2115 (w)
	UV/vis, λ (nm)[d]	504
B2	^{1}H NMR, δ (ppm)[a]	0.26 (s, 3H, Ru—CH₃), 2.0−2.2 (CH(C*H*₃)₂ and P—CH₃), 4.49 (sept, *J* = 6.6 Hz, 2H, C*H*(CH₃)₂), 8.45 (d, *J*(HH) = 7.8 1H, py—H),[e] 9.00 (s, 2H, N=CH)
	^{31}P NMR, δ (ppm)[a]	−8.5 (*P*Me₂Ph)
	IR ν(CO) (cm^{-1})[c]	1940 (s), 2032 (s), 2115 (w)
	UV/vis, λ (nm)[f]	480

[a] $CDCl_3$, T = 293 K. [b] Selected ^{13}C NMR data from the mixture **4a**, **13**, and **B1**. ^{13}C NMR: Ru(CO)₄(PMe₂Ph) (**13**) δ 204.1. [c] Selected from mixture; both in KBr pellet and CH_2Cl_2 solution. [d] Absorption of **4a** (λ 386 nm) also present. [e] Other pyridine signals obscured by PMe₂*Ph*₂. [f] Absorption of **4b** (λ = 363 nm) also present.

binuclear species, similar to the case of **2a** and **13** (vide supra). During the reaction of **4a** and **13** one major and two minor (<10%) species were observed by ^{1}H, ^{13}C, and ^{31}P NMR, which disappeared again at the end of the acylation reaction. The major species (**B1**) was formed in 45% yield directly after addition of **13** to **4a**. In Table 5 the NMR data of species **B1** are summarized. The ^{1}H and ^{13}C NMR data of **B1** show that the ruthenium—methyl bond (^{1}H NMR: δ 0.34 ppm) is still intact, and that the iPr-DAB ligand chelates σN,σN′ to a symmetric fragment. An interesting feature of **B1** is that the chemical shift of the phosphorus atom (^{31}P NMR: δ −8.8 ppm) is shifted to a higher field compared to Ru(CO)₄(PMe₂Ph) (^{31}P NMR: δ 11.5 ppm).[6] Since only terminal carbonyls were observed in ^{13}C NMR and IR, all data point to a structure in which the moieties Ru(CO)₄(PMe₂Ph) (**13**) and [Ru(CH₃)(CO)₂(iPr-DAB)][OTf] (**4a**) are linked together via a metal-to-metal donor bond (Scheme 5). The presence of a new band of low intensity in the UV spectrum (λ = 504 nm) on addition of the colorless solution of **13** to a yellow solution (λ = 386 nm) of **2a**, most probably stems from the ruthenium(II) to iPr-DAB transition, which has shifted to a lower energy as a result of the increased electron density on the Ru(II) center.[24]

When PPh₃ was added to this mixture of **4a**, **13**, and

(24) This band is most probably not due to a σ−σ* transition in the Ru—Ru bond, since these are generally of high extinction. (a) Tom Dieck, H.; Rohde, W.; Behrens, U. *Z. Naturforsch.* **1989**, *44B*, 158. (b) Nieuwenhuis, H. A.; Stufkens, D. J.; Oskam, A. Personal communication. The extinction coefficient of the Ru—Mn transition in Ru(CH₃)(CO)₂(α-diimine)Mn(CO)₅ is 13 000 and 9000 for α-diimine = iPr-DAB and iPr-Pyca, respectively.

B1 at 20 °C, the ^1H, ^{13}C, and ^{31}P NMR spectra showed that no acylated product **5a** had been formed, but quantitatively $[Ru(CH_3)(CO)_2(PPh_3)(iPr\text{-}DAB)][OTf]$ (**9a**) instead (Scheme 5). When on the other hand NEt_4I was added to a mixture of **4a**, **13**, and **B1** at 20 °C, $Ru(CH_3)I(CO)_2$(iPr-DAB) (**2a**) was formed very rapidly also in quantitative yield (Scheme 5). In both reactions **13** was again recovered (the reaction times are too short (1–5 min) for a reaction of **13** with PPh_3 or $CDCl_3$; vida infra). Since **4a** reacts with PPh_3 and NEt_4I to give **9a** and **2a**, respectively, it might well be that **B1** does not react with PPh_3 and NEt_4I but that the equilibrium simply shifts to **4a** and **13**. It should be noted that a direct reaction of **B1** with PPh_3 and I^- ions may of course take place also. The formation of **9a** and **2a** underlines that **B1** must be simply an addition product of **4a** and **13**. Whether **B1** is an intermediate to the acylation product **5a** is, however, not clear.

Coming back to the possibility of an ionic intermediate in the $Ru(CO)_4(PMe_2Ph)$ (**13**) promoted acylation of $Ru(CH_3)I(CO)_2$(iPr-DAB) (**2a**), we decided to carry out the acylation reaction with the chloride complex $Ru(CH_3)Cl(CO)_2$(iPr-DAB) (**6a**). Heating (45 °C) of a solution of **6a** in $CHCl_3$ under 1 atm of CO during 20 h resulted in the quantitative formation of the acyl product $Ru(C(O)CH_3)Cl(CO)_2$(iPr-DAB) (**7a**) (Table 4; Scheme 2). This acylation is much faster than for **2a**, most probably because of the dissociation of the chloride, which facilitates CO insertion, like in the case of the ionic complex $[Ru(CH_3)(CO)_2$(iPR-DAB)$][OTf]$ (**4a**). The easy dissociation of the chloride in $Ru(CH_3)Cl(CO)_2$(iPr-DAB) (**6a**) was proven by the fast quantitative formation of $[Ru(CH_3)(CO)_2$(iPr-DAB)$(PPh_3)][Cl]$ (**10a**) from **6a** and PPh_3 at 20 °C in $CDCl_3$ (Table 4). The rate of dissociation of the chloride in **6a** is much faster than of the iodide in **2a**, and the equilibrium **6a**/**10a** lies totally on the side of **10a** (at 20 and 45 °C) whereas the equilibrium **2a**/**8a** is 55/45 at 45 °C.

Reaction of $Ru(CH_3)Cl(CO)_2$(iPr-DAB) (**6a**) with $Ru(CO)_4(PMe_2Ph)$ (**13**) under 16 atm of CO pressure in $CDCl_3$ at 45 °C resulted in the quantitative formation of the acylated product $Ru(C(O)CH_3)Cl(CO)_2$(iPr-DAB) (**7a**) within 2 h, while complex **13** was recovered after this reaction time. The catalytic acylation of **6a** is slightly faster than that of **2a**. The reaction of **6a** with $Ru(CO)_4(PMe_2Ph)$ (**13**) and PPh_3 at 45 °C in $CDCl_3$ showed 55% conversion to $Ru(C(O)CH_3)Cl(CO)_2$(iPr-DAB) (**7a**) after 10 h and complete conversion of **13** to $[Ru(CO)_2(PMe_2Ph)(PPh_3)Cl]_2$ (**16**) (Table 4). ^1H and ^{31}P NMR spectra measured during the reaction reveal that in the beginning of the reaction both **6a** and **10a** are present (7/2) and that with decomposition of the catalyst, which consumes the triphenylphosphine, also complex **13** disappears. No intermediate of type **B1** was observed during this reaction. At the end of the reaction only **6a**, $Ru(C(O)CH_3)Cl(CO)_2$(iPr-DAB) (**7a**) (45/55), and **16** are present. The rate of acylation of **6a** and the side product formed in the beginning of the reaction are similar to that of **2a**, while the decomposition of **13** to form **16** was not observed for **2a** (vide infra). If, however, complex **6a** is reacted with $Ru(CO)_4(PMe_2Ph)$ (**13**) at 20 °C in $CDCl_3$, direct formation of an orange-red solution shows the formation of an intermediate of type **B**, i.e. $[Ru(CH_3)(CO)_2$(iPr-DAB)$Ru(CO)_4(PMe_2Ph)][Cl]$. Spectroscopic data confirm that an equilibrium between **6a**, **13**, and this species exists, since in the ^1H NMR spectrum several new signals are observed (spectrum too crowded for clear assignment), while the ^{31}P NMR spectrum shows a singlet at −8.82 ppm. For species **B1** and **B2**, the PPh_3 signal was observed at −8.8 and −8.5 ppm, respectively. In the ^{13}C NMR spectrum the signals of all carbons are broadened, which points to an exchange between the compounds **6a** and **13** and the adduct. However, the fact that none of these signals has been observed in the catalytic (**6a** and **13** under CO pressure) or in the stoichiometric (**6a** and **13** and PPh_3) acylation reaction strongly suggests that an intermediate adduct of type **B** is not an intermediate on the acylation pathway.

Deinsertion and C–H Activation in 2a and 3a. Kraakman reported the formation of $Ru(C(O)CH_3)I(CO)_2(CH(CH_3)_2{-}N{=}CHCH_2N{=}C(CH_3)_2)$ (**12**), in which a proton has shifted from the isopropyl group to the imine carbon atom in **3a**, upon refluxing **3a** with **13** in $CDCl_3$ without CO or PPh_3 (Scheme 1). We found, however, that refluxing of **2a** or **3a** in heptane for 20 h led to a mixture of **2a** and $Ru(CH_3)I(CO)_2(CH(CH_3)_2{-}N{=}CHCH_2N{=}C(CH_3)_2)$ (**11**) in a 4 to 1 ratio, showing that the presence of $Ru(CO)_4(PMe_2Ph)$ (**13**) is not needed to achieve C–H activation. The fact that only the methyl complex **11** is formed in the latter reaction is most probably because of the high temperature (120 °C) and long reaction time, which induces CO deinsertion.

$Ru(CO)_4(PMe_2Ph)$ (13) Assisted CO Insertion in $Ru(CH_3)X(CO)_2$(iPr-Pyca) (X = I (2b) and OTf (4b)). To obtain more information about the influence of the α-diimine on the carbonylation reaction, a series of $Ru(R)X(CO)_2$(R′-Pyca) complexes with R = CH_3 or acyl and R′ = isopropyl (**b**), methoxyethyl (**c**), and isopropoxypropyl (**d**) were synthesized. As was shown above, these complexes do not differ much in spectroscopic and structural properties. Therefore, only the $Ru(CO)_4(PMe_2Ph)$ assisted acylations of $Ru(CH_3)X(CO)_2$(iPr-Pyca) (X = I (**2b**); X = OTf (**4b**)) have been carried out and will be discussed here. The reactions have been summarized in Table 4.

Complex $Ru(CH_3)I(CO)_2$(iPr-Pyca) (**2b**) does not react with CO at low pressures. Under high pressures (16 atm) 40% of **2b** was converted to $Ru(C(O)CH_3)I(CO)_2$(iPr-Pyca) (**3b**) after 16 h at 45 °C, which is rather analogous to the behavior of the iPr-DAB complex **2a** (Table 4).[6]

The reaction of $Ru(CH_3)I(CO)_2$(iPr-Pyca) (**2b**) with $Ru(CO)_4(PMe_2Ph)$ (**13**) at 45 °C under 12 atm of CO pressure led to $Ru(C(O)CH_3)I(CO)_2$(iPr-Pyca) (**3b**) in 90% yield after 3.5 h (Table 4), which is somewhat slower than the same reaction with **2b**. It may well be that the slower rate of acylation of **2b** is a result of the decrease in catalyst concentration due to the decomposition of the catalyst **13** to form **15**.

The reaction of $Ru(CH_3)I(CO)_2$(iPr-Pyca) (**2b**) with $Ru(CO)_4(PMe_2Ph)$ (**13**) and PPh_3 in $CDCl_3$ at 45 °C led to formation of $Ru(C(O)CH_3)I(CO)_2$(iPr-Pyca) (**3b**) (17%) and to $[Ru(CH_3)(CO)_2(PPh_3)$(iPr-Pyca)$][I]$ (**8b**) (27%) after 17 h, while $Ru(CO)_4(PMe_2Ph)$ (**13**) decomposed with formation of $[Ru(CO)_2(PMe_2Ph)(PPh_3)Cl]_2$ (**16**) (Scheme 6; Table 4). The acylation of **2b** in the presence of **13** and PPh_3 in $CDCl_3$ at 45 °C is slower (27% conversion to **3b** after 17 h) than that of **2a** (complete conversion to **3a** after 17 h). Since the concentration of the catalyst **13** decreases much faster in the case of **2b** than of **2a** as a result of decomposition, the rates

Scheme 6. Reactions of Ru(CH$_3$)I(CO)$_2$(iPr-Pyca) (2b) with Ru(CO)$_4$(PMe$_2$Ph) (13) and PPh$_3$

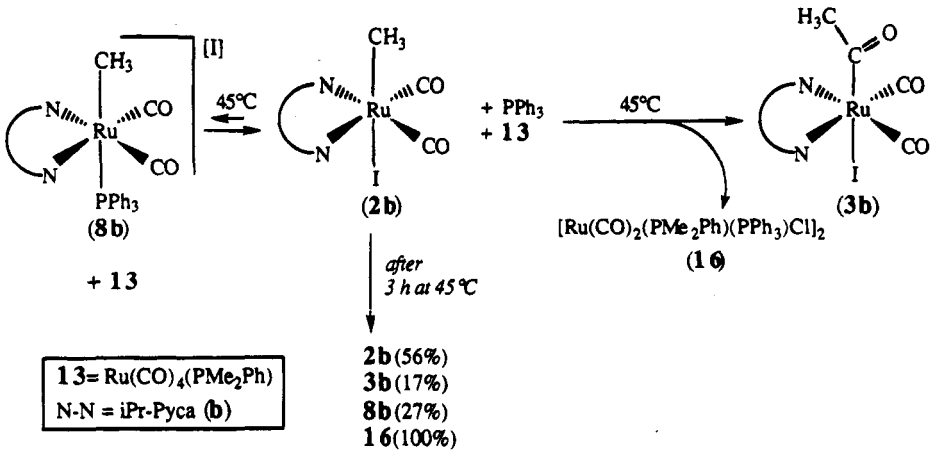

cannot be compared. During the reaction of **2b**, **13**, and PPh$_3$ two species were observed, of which the ^{1}H and ^{31}P NMR spectra resembled those of the species observed in the reaction of **2a**, **13**, and PPh$_3$. The major species (present in ca. 25% during the reaction) is [Ru(CH$_3$)(CO)$_2$(PPh$_3$)(iPr-Pyca)][I] (**8b**) (Scheme 6; Table 4). The fact that **8b** is still present (27%) after 17 h of reaction time is a result of the incomplete conversion of **2b** to **3b**. In the case of **2a** intermediate **8a** disappears again when all **2a** is converted to **3a** (vide supra).

Complex **2b** did not react with PPh$_3$ in CDCl$_3$ at 20 °C. At 45 °C only 10% of **2b** was converted to [Ru(CH$_3$)(CO)$_2$(PPh$_3$)(iPr-Pyca)][I] (**8b**) after 4 h, which indicates that iodide dissociation from **2b** is slower than for **2a** (Scheme 6; Table 4). The reaction of **2b** with Ru(CO)$_3$(PMe$_2$Ph) (**13**) in the absence of PPh$_3$ at 45 °C in CDCl$_3$ yielded 16% of **3b** after 3 h, together with an unknown species (11%).

Refluxing of Ru(C(O)CH$_3$)I(CO)$_2$(iPr-Pyca) (**3b**) for 18 h in heptane resulted in the quantitative re-formation of **2b**. The deinsertion of CO is quantative for both **3a** and **3b**, although for complex **3a** also C—H activation was observed (vide supra). Apparently the C—H activation is not favored for the iPr-Pyca complex **3b**, possibly because of the more rigid N=C—C=N frame.

Reaction of [Ru(CH$_3$)(CO)$_2$(iPr-Pyca)][OTf] (**4b**) with Ru(CO)$_4$(PMe$_2$Ph) (**13**) in CDCl$_3$ yielded [Ru(C(O)CH$_3$)(CO)$_2$(iPr-Pyca)][OTf] (**5b**) within 3 h, together with [Ru(CO)$_2$(PMe$_2$Ph)Cl]$_2$ (**15**) (Scheme 5; Table 4). NMR, IR, and UV/vis spectroscopy revealed the presence of an intermediate complex **B2** in circa 45% yield, which is formed directly after addition of **13** to **4b**. Addition of PPh$_3$ to a fresh solution of **4b**, **13**, and **B2** afforded within 5 min [Ru(CH$_3$)(CO)$_2$(PPh$_3$)(iPr-Pyca)][OTf] (**9b**) and **13** similar to the case of **4a** and **13**. The spectroscopic data for **B2** (Table 5) suggest that the structure of **B2** is similar to that of **B1**. Again only terminal CO's are observed in the IR and the methyl-ruthenium is still present (δ 0.26 ppm in ^{1}H NMR). For the mixture of **4b**, **13**, and **B2** the UV/vis spectrum shows bands at 354 and 480 cm^{-1}, together with the band at 363 cm^{-1} from **4b**.

In the reaction of [Ru(CH$_3$)(CO)$_2$(iPr-Pyca)][OTf] (**4b**) with Ru(^{13}CO)$_4$(PMe$_2$Ph) (**13**) ^{13}CO enrichment of both the carbonyl groups and the acyl group in [Ru(C(O)CH$_3$)(CO)$_2$(iPr-Pyca)][OTf] (**5b**) was observed, as in the case of **4a** (vide supra). To check whether ^{13}CO scrambling was a result of the reversible formation of a binuclear species, RuI$_2$(CO)$_2$(iPr-Pyca) (**1b**) was stirred several days under a ^{13}CO atmosphere at 45 °C. In this case no scrambling of CO was observed. However, stirring of **1b** with Ru(^{13}CO)$_4$(PMe$_2$Ph) (**13**) at 45 °C resulted in significant ^{13}CO incorporation in both the carbonyl groups of **1b**, as in the case of **1a** (vide supra).

The analogous observations for complexes **2a** and **4a** and complexes **2b** and **4b**, respectively, strongly suggest that the mechanisms for CO scrambling and CO insertion are very similar for complexes containing iPr-DAB (**a**) and iPr-Pyca (**b**), with the intermediacy of bimetallic intermediates on the route to the acylated products.

Conversion of Ru(CO)$_4$(PMe$_2$Ph) (13). A rather intriguing observation is that in CDCl$_3$ both Ru(CO)$_4$(PMe$_2$Ph) (**13**) and Ru(CO)$_3$(PMe$_2$Ph)(PPh$_3$) (**14**) are only stable in the presence of Ru(CH$_3$)I(CO)$_2$(iPr-DAB) (**2a**), Ru(CH$_3$)Cl(CO)$_2$(iPr-DAB) (**6a**), and Ru(CH$_3$)I(CO)$_2$(iPr-Pyca) (**2b**) under CO pressure (>8 atm), while **13** alone is not stable in CDCl$_3$ at 45 °C under CO pressure. Therefore, it appeared to us imperative to study the stability and reactivity of **13** itself in various solvents. It turned out that complex **13** is stable in hexane, CH$_2$Cl$_2$, and THF, both at 20 and 45 °C under N$_2$ and under a CO atmosphere, according to ^{31}P NMR (IR revealed that after 2 h at 45 °C under a N$_2$ atmosphere some decomposition had taken place in all solvents). It was reported that the analogous complexes Ru(CO)$_4$(PR)$_3$ with PR$_3$ = PPh$_3$, PMePh$_2$, and PnBu$_3$ decomposed due to CO loss, even in the solid state.[11a] Complex Ru(CO)$_4$(PMe$_2$Ph) (**13**) is stable for several weeks when stored at −20 °C. However, when a solution of **13** is stirred in the absence of CO for 18 h at 20 °C or for 2 h at 45 °C in CHCl$_3$ or CDCl$_3$ the colorless solution turned completely yellow with the formation of Ru$_2$(CO)$_4$(PMe$_2$Ph)$_2$(μ-Cl)$_2$ (**15**), as shown by IR and ^{31}P NMR spectroscopy. Complex **15** has a structure analogous to those of Ru$_2$(CO)$_4$(PPh$_3$)$_2$(μ-I)$_2$[25] and [Ru$_2$(CO)$_4$((PtBu$_3$)$_2$(μ-Cl)$_2$,[26] which both contain bridging halide ions. Additional confirmation of the proposed structure is provided by the reaction of **15** with PPh$_3$, or by reaction of **13** with PPh$_3$ in CDCl$_3$ for 24 h, which afforded Ru$_2$(CO)$_4$(PMe$_2$Ph)$_2$(PPh$_3$)$_2$(μ-Cl)$_2$ (**16**) (Scheme 7). Complex **16** shows two doublets in the ^{31}P NMR (δ = 5.2 and 16.6 ppm) with a large P—P coupling (343 Hz), which indicates that the PMe$_2$Ph and PPh$_3$ groups

(25) (a) Jungbluth, H.; Stöckli-Evans, H.; Süss-Fink, G. *J. Organomet. Chem.* **1989**, *377*, 339. (b) Jones, D. F.; Dixneuf, P. H. *J. Organomet. Chem.* **1981**, *210*, C41.

(26) Schumann, H.; Opitz, J.; Pickardt, J. *Chem. Ber.* **1980**, *113*, 1385.

Scheme 7. Conversion Products of $Ru(CO)_4(PMe_2Ph)$ (13)

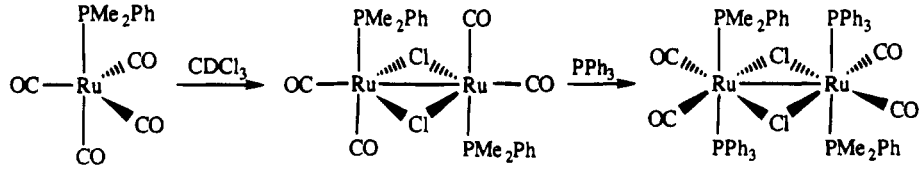

(13) (15) (16)

are coordinated trans toward each other.[27] In the mass spectrum of **16** (M = 1186 amu) a signal at half the mass of **16** (*m/e* 593) was observed, which is quite common for dimeric species of this type.

The tendency to form **15** from **13** is rather strong, since **13** is converted in $CDCl_3$ at both 1 and 8 atm of CO at 45 °C to **15** within 2 h, while **13** is stable in CH_2Cl_2, THF, and hexane under N_2 at 45 °C. Since **13** could be rapidly enriched with ^{13}CO in hexane at 45 °C,[6] it is clear that CO dissociates easily. The formation of **15** from **13** in $CDCl_3$ even under CO, can be rationalized by the formation of the coordinatively unsaturated species $[Ru(CO)_3(PMe_2Ph)]$, which may be attacked by $CDCl_3$ and forms via oxidative addition complex **15**. It is understandable that complex **13** is stable in THF and hexane, while it is rather surprising that **13** is also stable in CH_2Cl_2, even in the absence of CO. This might be due to the more polar character of CH_2Cl_2 which therefore acts as a stabilizing ligand to unsaturated zerovalent ruthenium species. A final interesting point is that in the presence of PPh_3 complex **13** sluggishly reacts in $CDCl_3$ to form $Ru(CO)_3(PMe_2Ph)(PPh_3)$ (**14**) but rapidly to form **14** in CH_2Cl_2 and THF, for which we have no ready explanation.

Stabilizing Effect of Complex $Ru(CH_3)X(CO)_2$(α-diimine) (2a, 6a, 2b) on 13 in $CDCl_3$ under a CO Atmosphere. In view of the behavior of $Ru(CO)_4(PMe_2Ph)$ (**13**) in $CDCl_3$ it is at first sight rather astonishing that during the reaction of **2a**, **6a**, or **2b** with **13** under 8–16 atm of CO in $CDCl_3$ at 45 °C, even at higher concentrations of **13**, complex **13** is not converted (**2a**, **6a**) or only in 5–10% converted (**2b**) to the dimeric Ru(II) complex **15**. Also when no CO is present, but instead PPh_3, acylation of **2a** occurs to form **3a**, while **13** is converted to $Ru(CO)_3(PMe_2Ph)(PPh_3)$ (**14**) and not to the dimeric Ru(II) complex. We may therefore conclude that the rate of reaction of $Ru(CO)_4(PMe_2Ph)$ (**13**) or most likely $[Ru(CO)_3(PMe_2Ph)]$ is faster with **2a**, **6a**, or **2b** than with $CDCl_3$, which is indeed slow, as shown in the previous section.

The fact that the ionic complexes $[Ru(CH_3)(CO)_2$(iPr-DAB)] (**4a**) and $[Ru(CH_3)(CO)_2$(iPr-DAB)] (**4b**) do not stabilize $Ru(CO)_4(PMe_2Ph)$ (**13**) is easily understood, since the ionic complexes **4a** and **4b** take away a carbonyl ligand from **13** to form the acyl complexes **5a** and **5b**, and there is no CO present to fill up the empty coordination site in $[Ru(CO)_3(PMe_2Ph)]$.

(27) Verkade, J. G., Quin, L. D., Eds. *Phosphorus-31 NMR spectroscopy in stereochemical analysis*; VCH Publishers: Dearfield Beach, FL, 1987.

Conclusions

In this paper we have studied in much greater detail the complicated $Ru(CO)_4(PMe_2Ph)$ (**13**) promoted acylation reaction of $Ru(CH_3)I(CO)_2$(iPr-DAB) (**2a**) and furthermore the carbonylation of the related complexes $Ru(CH_3)Cl(CO)_2$(iPr-DAB) (**6a**) and $Ru(CH_3)I(CO)_2$(iPr-Pyca) (**2b**). The observed reactivity of the complexes **2a**, **6a**, and **2b** is very similar, as is the reactivity of $[Ru(CH_3)(CO)_2$(iPr-DAB)][OTf] (**4a**) and $[Ru(CH_3)(CO)_2$(iPr-Pyca)[OTf] (**4b**). For complexes **2a**, **6a**, and **2b** the same number of species are observed during the reaction with **13** and PPh_3. The main species was shown to be the ionic phosphine complex $[Ru(CH_3)(CO)_2(PPh_3)$(α-diimine)][X], which is, however, not an intermediate on the acylation pathway.

The reaction of the ionic species $[Ru(CH_3)(CO)_2$(α-diimine)][OTf] (**4a**, **4b**) or the chloride complex $Ru(CH_3)Cl(CO)_2$(iPr-DAB) (**6a**) with **13** at 20 °C resulted in the formation of an adduct species (45%), most probably $[Ru(CH_3)(CO)_2$(α-diimine)$Ru(CO)_4(PMe_2Ph)][X]$ (**B**: X = OTf, Cl). This adduct species **B** is most probably not an intermediate on the acylation pathway.

By ^{13}CO labeling experiments it has clearly been demonstrated that binuclear species are involved in the reaction, most probably of the type $[Ru(CH_3)X(CO)Ru(CO)_3(PMe_2Ph)(\mu\text{-}CO)_2]$ (**X1**). The active species must be present in a very low concentration, since no binuclear compound with bridging carbonyl ligands could be detected by NMR or IR spectroscopy.

Complex $Ru(CO)_4(PMe_2Ph)$ (**13**), which was used as a carbonyl source for the acylation reaction decomposed at 45 °C in $CDCl_3$ to form $Ru_2(CO)_4(PMe_2Ph)_2(\mu\text{-}Cl)_2$ (**15**), or $Ru_2(CO)_4(PMe_2Ph)_2(PPh_3)_2(\mu\text{-}Cl)_2$ (**16**), when PPh_3 was present. The stability of **13** under high CO pressure in the presence of **2a**, **6a**, and **2b** in $CDCl_3$ at 45 °C for several hours, while **13** itself decomposes under these conditions, is most probably due to the faster reaction of $Ru(CO)_4(PMe_2Ph)$ (**13**) or most likely $[Ru(CO)_3(PMe_2Ph)]$ with **2a**, **6a**, or **2b** than with $CDCl_3$.

Acknowledgment. The *Netherlands Foundation for Chemical Research (SON)* and the *Netherlands Organization for Scientific Research (NWO)* are thanked for financial support (BdK-E). We owe thanks to *Johnson Matthey Inc.* for a loan of $RuCl_3 \cdot 3H_2O$.

Supplementary Material Available: Tables of atomic coordinates, thermal parameters, and bond distances and angles for **4c** (5 pages). Ordering information is given on any current masthead page. Further details of the crystal structure determination are available from the authors on request.

OM940079E